

Hurricane Effects on Neotropical Lizards Span Geographic and Phylogenetic Scales

Donihue, C. M., A. M. Kowaleski, J. B. Losos, A. C. Algar, S. Baeckens, R. W. Buchkowski, A.-C. Fabre, H. K. Frank, A. J. Geneva, R. G. Reynolds, J. T. Stroud, J. A. Velasco, J. J. Kolbe, D. L. Mahler, and A. Herrel. 2020.

Published online: 27/04/2020

Proceedings of the National Academy of Sciences:202000801.

DOI: [10.1073/pnas.2000801117](https://doi.org/10.1073/pnas.2000801117)

The version here is the accepted verison, the publishe version is available at:

<https://doi.org/10.1073/pnas.2000801117>

1 Classification: Biological Sciences: Evolution

2

3

4 **Hurricane Effects on Neotropical Lizards Span Geographic and Phylogenetic Scales**

5

6

7 C.M. Donihue^{1*}, A. Kowaleski², J.B. Losos^{1,3}, A.C. Algar⁴, S. Baeckens^{5,6}, R.W.
8 Buchkowski⁷, A.-C. Fabre⁸, H.K. Frank^{9,10}, A.J. Geneva^{1,11}, R.G. Reynolds¹², J.T. Stroud¹,
9 J.A. Velasco¹³, J.J. Kolbe¹⁴, D.L. Mahler¹⁵, A. Herrel^{5,16,17}

10 ¹Department of Biology, Washington University in St. Louis, St. Louis MO, USA

11 ²Department of Meteorology and Atmospheric Science, The Pennsylvania State University,
12 University Park PA, USA

13 ³ Living Earth Collaborative, Washington University in St. Louis, St. Louis MO, USA

14 ⁴ School of Geography, University of Nottingham, Nottingham NG7 2RD, UK

15 ⁵ Functional Morphology Lab, Department of Biology, University of Antwerp Wilrijk, BE

16 ⁶ Department of Biological Science, Macquarie University, Sydney, AU

17 ⁷ School of Forestry & Environmental Studies, Yale University, New Haven CT, USA

18 ⁸ Department of Life Sciences, The Natural History Museum, London, UK

19 ⁹ Department of Pathology, Stanford University, Stanford CA, USA

20 ¹⁰ Department of Ecology and Evolutionary Biology, Tulane University, New Orleans, LA, USA

21 ¹¹ The Academy of Natural Sciences of Drexel University, Philadelphia PA, USA

22 ¹² Department of Biology, University of North Carolina Asheville, Asheville NC, USA

23 ¹³ Centro de Ciencias de la Atmósfera, Universidad Nacional Autónoma de México, Mexico
24 City, MX

25 ¹⁴ Department of Biological Sciences, University of Rhode Island, Kingston RI, USA

26 ¹⁵ Department of Ecology of Ecology and Evolutionary Biology, University of Toronto, Toronto
27 ON, CA

28 ¹⁶ UMR7179, CNRS/MNHN, 55 rue Buffon, Paris, FR

29 ¹⁷ Evolutionary Morphology of Vertebrates, Ghent University, K. L. Ledeganckstraat 35, Ghent,
30 BE

31

32 *Correspondence author: Colin M. Donihue, Department of Biology, Washington University in
33 St. Louis, St. Louis MO, USA; colindonihue@gmail.com

34 **Extreme climate events such as droughts, cold snaps, and hurricanes can be**
35 **powerful agents of natural selection, producing acute selective pressures very different**
36 **from the everyday pressures acting on organisms. Yet, it remains unknown whether these**
37 **infrequent but severe disruptions are quickly erased by quotidian selective forces, or**
38 **whether they have the potential to durably shape biodiversity patterns across regions and**
39 **clades. Here, we show that hurricanes have enduring evolutionary impacts on the**
40 **morphology of anoles, a diverse Neotropical lizard clade. We first demonstrate a trans-**
41 **generational effect of extreme selection on toepad area for two populations struck by**
42 **hurricanes in 2017. Given this short-term effect of hurricanes, we then asked whether**
43 **populations and species that more frequently experienced hurricanes have larger toepads.**
44 **Using 70 years of historical hurricane data, we demonstrate that, indeed, toepad area**
45 **positively correlates with hurricane activity for both 12 island populations of *Anolis sagrei***
46 **and 188 *Anolis* species throughout the Neotropics. Extreme climate events are intensifying**
47 **due to climate change and may represent overlooked drivers of biogeographic and large-**
48 **scale biodiversity patterns.**

49

50 Keywords: Cyclones, Extreme Climate Events, Rapid Evolution, *Anolis*

51

52 **Significance statement:** Extreme climate events can act as agents of natural selection. We
53 demonstrate that lizards hit by Hurricanes Irma and Maria in 2017 passed on their large, strong-
54 gripping toepads to the next generation of lizards. Moreover, we found that across 12 insular
55 populations of *A. sagrei*, and 188 *Anolis* species across the neotropics, those hit by more
56 hurricanes in the last 70 years tended to have proportionately larger toepads. Our study suggests

57 that hurricanes can have long-term and large-scale evolutionary impacts that transcend
58 biogeographic and phylogenetic scales. As hurricanes become more severe due to climate
59 change, these extreme climate events may have a much larger impact on the evolutionary
60 trajectory of the affected ecological communities than previously appreciated.

61

62

63

64 Extreme climate events can be powerful agents of natural selection, but their
65 consequences for large-scale biodiversity patterns are relatively unknown (1–3). Some theory
66 predicts that infrequent, extreme selection events on ecological timescales will not have long-
67 lasting evolutionary impacts on species (4). Few empirical studies have tested this prediction
68 because extreme climate events are intrinsically rare (1, 5). Testing the long-term evolutionary
69 effects of extreme climate events requires investigating two propositions: first, that extreme
70 events actually impose strong selection and, second, that the evolutionary response to this
71 selection is durable enough to shape large scale diversity patterns. To date, such data only exist
72 for Darwin’s finches on a small, isolated island (6). There, researchers observed that extreme wet
73 or dry years drive strong selection, but that alternating extreme climate events reverse the
74 direction of selection and erase the evolutionary trends on decadal timescales (6). An alternative
75 approach to tracking evolutionary change over time is to compare it over space, with the
76 prediction that if extreme events have long-lasting impact, then populations in areas more often
77 affected by such events will exhibit traits different from those in less-affected areas. Here, we
78 pair a cross-generational and spatial approach to investigate the evolutionary impact of
79 hurricane-induced selection.

80 Immediately following Hurricanes Irma and Maria in 2017, we documented rapid,
81 directional shifts in morphology in two island populations of a Caribbean anole (*Anolis scriptus*)
82 in the Turks and Caicos Islands (TCI) (3). We found that post-hurricane populations had larger
83 subdigital toepads—a key trait in anoles responsible for clinging performance (3, 7). However, it
84 remained unclear whether this selection would lead to persistent phenotypic differences in the
85 population through time.

86 In 2019, we revisited the *A. scriptus* populations on Pine and Water Cays (TCI) to
87 determine whether the hurricane effect had persisted in the 18 months following the initial
88 selective event. We resurveyed the populations following the same methods used in 2017 (see
89 Methods). The relative surface areas of the fore- and hind limb toepads of the populations
90 measured 18 months after the hurricanes were statistically indistinguishable from those of the
91 hurricane survivors (forelimb: $\beta \pm \text{s.e.}: -0.009 \pm 0.006$, $t_{290} = -1.37$; $P = 0.1709$; hind limb: $\beta \pm$
92 $\text{s.e.}: -0.007 \pm 0.006$, $t_{291} = -1.278$; $P = 0.2024$), and remained significantly larger than those of
93 the pre-hurricane populations (forelimb: $\beta \pm \text{s.e.}: 0.050 \pm 0.007$, $t_{290} = 7.117$; $P < 0.0001$; hind
94 limb: $\beta \pm \text{s.e.}: 0.038 \pm 0.006$, $t_{291} = 6.074$; $P < 0.0001$; Fig. 1; all analyses corrected for body
95 size). Moreover, these patterns of selection (3) and persistence (shown here) were parallel across
96 both island populations (see Appendix 1 for full model output).

97 To test whether these trait shifts transcended generations, we further analyzed these data,
98 restricting the analyses to those individuals measured in 2019 that, based upon estimated growth
99 rates, most likely hatched after the hurricane and thus were offspring of hurricane survivors
100 (Supplemental Information). Results were unchanged: the relative surface area of the toepads of
101 these next-generation lizards was indistinguishable from that of the hurricane survivors
102 (forelimb: $\beta \pm \text{s.e.}: -0.006 \pm 0.018$, $t_{267} = -0.332$; $P = 0.7401$; hind limb: $\beta \pm \text{s.e.}: -0.011 \pm 0.015$,

103 $t_{269} = -0.711$; $P = 0.4774$), and remained significantly larger than the pre-hurricane populations
104 (forelimb: $\beta \pm \text{s.e.}: 0.124 \pm 0.020$, $t_{267} = 6.086$; $P < 0.0001$; hind limb: $\beta \pm \text{s.e.}: 0.093 \pm 0.017$,
105 $t_{269} = 5.246$; $P < 0.0001$; Fig. 1). The shifts were parallel on the two islands and robust for
106 different growth rate estimates (Appendix 1).

107 These results demonstrate that changes following a catastrophic selective event were
108 maintained over the short term. To test whether such events have longer-term impacts, we
109 broadened our sampling and investigated whether variation in hurricane history across space
110 correlated with variation in toepad characteristics at two geographical scales: within a single
111 wide-spread species found on many Caribbean islands, and across the range of the *Anolis* genus.

112 To do so, we surveyed populations of the brown anole (*A. sagrei*), a species that is
113 similar in ecology and morphology to *A. scriptus* (8). Across 12 islands that span the natural
114 range of *A. sagrei* from the Bahamas to the Cayman Islands, the number of hurricane events in
115 the preceding 70 years significantly predicted the surface area of an island population's toepads
116 (forelimb: $\beta \pm \text{s.e.}: 0.050 \pm 0.018$, $t_9 = 2.878$; $P = 0.0182$; hind limb: $\beta \pm \text{s.e.}: 0.055 \pm 0.014$, $t_9 =$
117 3.881 ; $P = 0.0037$; Fig. 2; analyses accounted for body size and phylogenetic non-independence;
118 see Methods for hurricane activity calculations and Appendix 2 for full model output). Island
119 populations of *A. sagrei* that experienced more hurricanes have relatively larger toepads than
120 those that experienced fewer hurricanes.

121 We next investigated whether the hurricane-driven pattern would hold true across the
122 distribution of the *Anolis* genus as a whole. We measured toepad size for 188 species of *Anolis*
123 lizards across the clade's distribution (Fig. 3). Species that experienced more hurricanes had
124 relatively larger toepads on both forelimbs ($\beta \pm \text{s.e.}: 0.061 \pm 0.012$, $t_{165} = 5.031$; $P < 0.0001$) and
125 hind limbs ($\beta \pm \text{s.e.}: 0.050 \pm 0.013$, $t_{165} = 3.90$; $P = 0.0001$; Fig 3; analyses accounted for body

126 size and phylogenetic non-independence; Appendix 3). We tested additional potential
127 explanatory variables across the range of the anoles including local maximum tree height, air
128 temperature, and precipitation and found no significant correlations with toepad area (Appendix
129 4, Appendix 5). Eliminating mainland species – which typically experience fewer hurricanes
130 than their insular counterparts – yielded a similar positive relationship (forelimb: $\beta \pm \text{s.e.}: 0.056$
131 ± 0.013 , $t_{121} = 4.467$; $P < 0.0001$; hind limb: $\beta \pm \text{s.e.}: 0.048 \pm 0.012$, $t_{121} = 3.882$; $P = 0.00017$;
132 Appendix 3).

133 The correlation between toepad surface area and hurricane activity seen among
134 populations of *A. sagrei* and across Neotropical *Anolis* could arise in two ways. On one hand,
135 selection for larger toepads, as seen in *A. scriptus* in the Turks and Caicos, may have long-lasting
136 consequences that are not erased by different selection pressures in periods between hurricanes.
137 Alternatively, hurricanes may change the environment in ways that change selection pressures in
138 subsequent years when hurricanes don't occur. However, given that hurricane-prone areas tend
139 to have shorter trees (Appendix 4) and that a general positive correlation between perch height
140 and toepad area exists (8), one might expect hurricane-prone areas to have smaller toepads, the
141 opposite of the trend we observed. More detailed analysis of how hurricanes affect vegetation
142 structure vis-à-vis anole habitat use, as well as long-term selection studies, are needed to clarify
143 this mechanism.

144 Our demonstration that rare but extreme events can impact evolution raises the further
145 question of what role such events play in shaping phylogenetic patterns of trait diversity
146 compared to other selective factors. Caribbean anoles are an excellent group in which to
147 investigate this pattern because of the well-documented replicated patterns of adaptive radiation
148 across Greater Antillean islands (8, 9). Anoles have repeatedly diverged into multiple habitat

149 specialist types, termed ecomorphs, that differ in morphological traits related to habitat use. In
150 the context of this adaptive divergence, we can ask what effect hurricane activity has on this
151 variation in relative toepad surface area. For all ecomorphs, species in areas more frequently hit
152 by hurricanes have larger toepads (Appendix 3). One might predict that the effect of hurricanes
153 would differ among habitats—more arboreal species, for example, might be more exposed to the
154 storm’s force. Our analyses, however, find that the response to hurricanes was consistent and
155 positive across habitat specialist types (Appendix 3). Moreover, hurricane activity explains a
156 substantial portion of variation in relative toepad area (Table 1), revealing a hitherto unsuspected
157 driver of anole diversity and demonstrating that extreme events can be a major contributor to
158 phenotypic diversity patterns at large phylogenetic and biogeographic scales.

159 More remains to be discovered about how variation in hurricane attributes (e.g., storm
160 duration, prevailing direction, accompanying rain) affects the concurrent and post-hurricane
161 selective landscape for anoles. A preliminary analysis found no relationship between time since
162 last hurricane and toepad area in our *A. sagrei* samples (Appendix 2.2); however, repeated
163 sampling following storms is needed to fully address this question. Moreover, toepads are only
164 one of several traits in anoles linked to clinging capacity, and so future work comparing limb
165 morphology (10) and claw shape (11, 12) may yet reveal new insights into the biomechanical
166 predictors of survivorship during storms (13, 14) and the clade-wide impacts of hurricanes on the
167 morphology in this genus.

168 Hurricanes are intensifying due to climate change (15–17) and can be powerful agents of
169 natural selection (3). As such, they may represent overlooked drivers of biogeographic and
170 phylogenetic patterns, necessitating a global, cooperative effort to determine their ecological and
171 evolutionary effects (18). For anoles, hurricanes are severe selective events, leading to

172 population-level changes in morphology that persist across generations. Moreover, as evidenced
173 by the relationship between toepad surface area and hurricane activity within and among *Anolis*
174 species, hurricanes can have long-lasting evolutionary effects. Our study therefore demonstrates
175 that extreme climate events can have enduring evolutionary impacts that transcend phylogenetic
176 and geographic scales.

177 **References and Notes:**

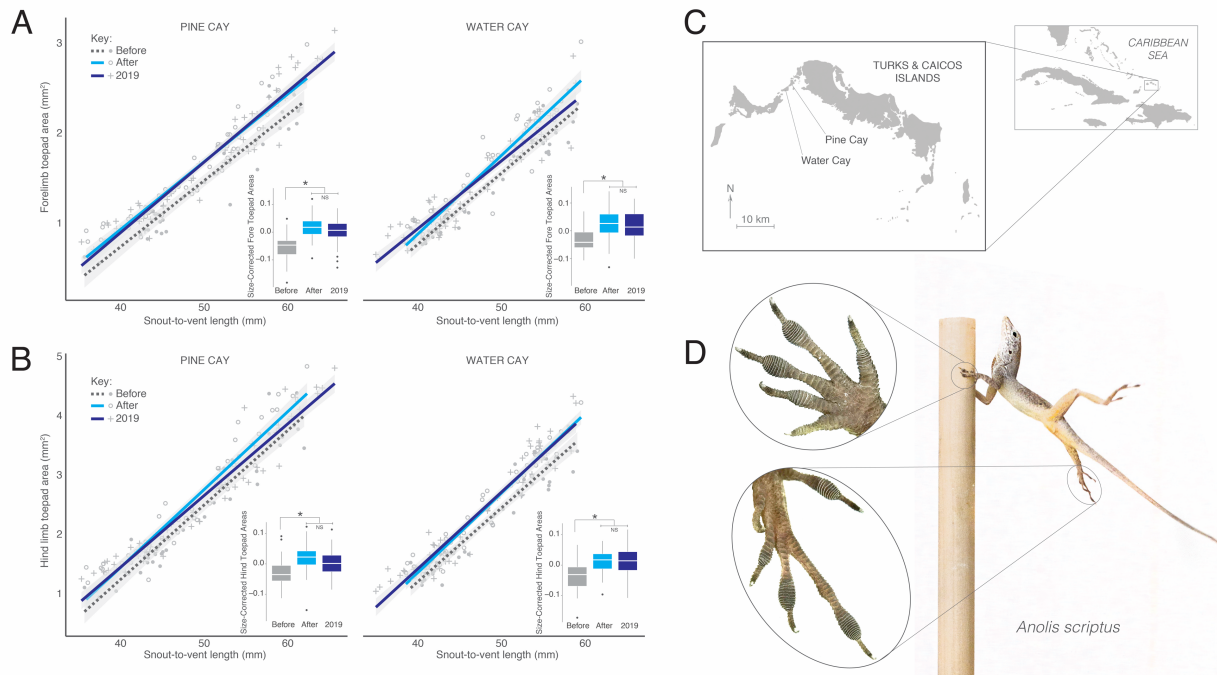
- 178 1. P. R. Grant, B. R. Grant, R. B. Huey, M. T. J. Johnson, A. H. Knoll, J. Schmitt, Evolution
179 caused by extreme events. *Phil. Trans. R. Soc. B* 372, 20160146 (2017).
- 180 2. S. C. Campbell-Staton, Z. A. Cheviron, N. Rochette, J. Catchen, J.B. Losos, S. V. Edwards,
181 Winter storms drive rapid phenotypic, regulatory, and genomic shifts in the green anole
182 lizard. *Science* 357, 495-498 (2017).
- 183 3. C. M. Donihue, A. Herrel, A.-C. Fabre, A. Kamath, A. J. Geneva, T. W. Schoener, J. J.
184 Kolbe, J. B. Losos, Hurricane-induced selection on the morphology of an island lizard.
185 *Nature* 560, 88-91 (2018).
- 186 4. S. J. Gould, The paradox of the first tier: an agenda for Paleobiology. *Paleobiology* 11, 2-12
187 (1985).
- 188 5. P. R. Grant, Evolution, climate change, and extreme events. *Science* 357, 451-452 (2017).
- 189 6. P. R. Grant, B. R. Grant, Unpredictable evolution in a 30-year study of Darwin's finches.
190 *Science* 296, 707-711 (2002).
- 191 7. D. J. Irschick, A. Herrel, B. Vanhooydonck, Whole-organism studies of adhesion in pad-
192 bearing lizards: creative evolutionary solutions to functional problems. *J. Comp. Physiol. A*.
193 192, 1169-1177 (2006).
- 194 8. J. B. Losos, Lizards in an evolutionary tree: ecology and adaptive radiation of anoles (Univ.
195 of California Press, Berkeley, 2009).
- 196 9. E. E. Williams, The origin of faunas. Evolution of lizard congeners in a complex island
197 fauna: A trial analysis. *Evol. Biol.* 6, 47-89 (1972).
- 198 10. J. Kolbe, Effects of hind-limb length and perch diameter on clinging performance in *Anolis*
199 lizards from the British Virgin Islands. *J. Herp.* 49, 284-290 (2015).
- 200 11. P. A. Zani, The comparative evolution of lizard claw and toe morphology and clinging
201 performance. *J. Evol. Biol.* 13, 316-325 (2000).
- 202 12. K. E. Crandell, A. Herrel, M. Sasa, J. B. Losos, K. Autumn, Stick or grip? Co-evolution of
203 adhesive toepads and claws in *Anolis* lizards. *Zoology* 117, 363-369 (2014).
- 204 13. M. Denny, Extreme drag forces and the survival of wind- and water-swept organisms. *J. Exp.*
205 *Biol.* 194, 97-115 (1994).
- 206 14. M. Denny, Predicting physical disturbance: Mechanistic approaches to the study of
207 survivorship on wave-swept shores. *Ecol. Monographs* 65, 371-418 (1995).
- 208 15. G. C. Hegerl, H. Hanlon, C. Beierkuhnlein, Climate science: elusive extremes. *Nat. Geosci.*
209 4, 142-143 (2011).
- 210 16. A. H. Sobel, S. J. Camargo, T. M. Hall, C.-Y. Lee, M. K. Tippett, A. A. Wing, Human
211 influence on tropical cyclone intensity. *Science* 353, 242-246 (2016).
- 212 17. K. J. E. Walsh, J. L. McBride, P. J. Klotzbach, S. Balachandran, S. J. Camargo, G. Holland,
213 T. R. Knutson, J. P. Kossin, T. Lee, A. Sobel, M. Sugi, Tropical cyclones and climate
214 change. *Wire's Climate Change* 7, 65-89 (2016).

215 18. J. N. Pruitt, A. G. Little, S. J. Majumadar, T. W. Schoener, D. N. Fisher, Call-to-action: A
216 global consortium for tropical cyclone ecology. *Trends Ecol. Evol.* 34, 588-590 (2019).

Factor	Forelimb R²	Hind Limb R²
Hurricane Activity + Ecomorph	0.50	0.40
Hurricane Activity	0.19	0.11
Ecomorph	0.29	0.26

217

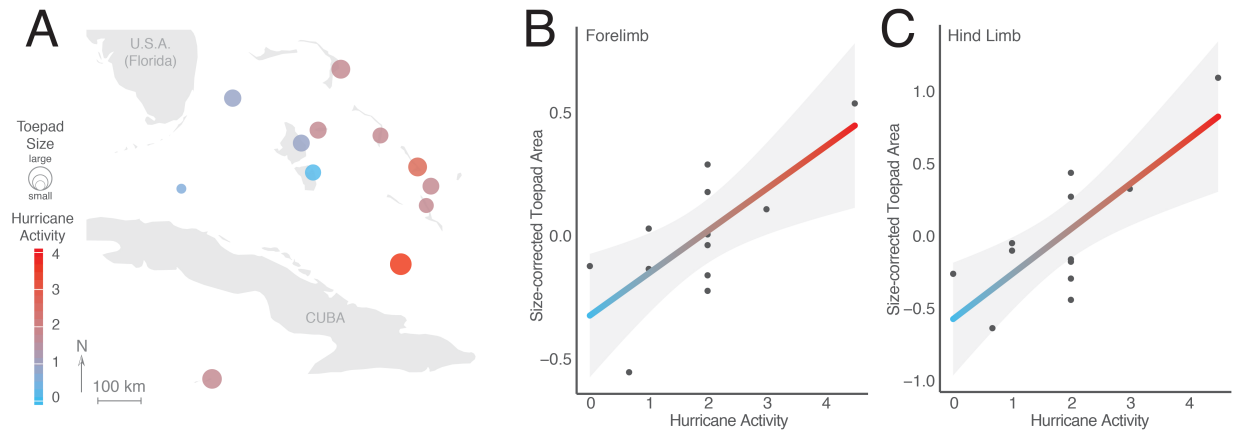
218 **Table 1:** The explanatory power of ecomorph class and historical hurricane activity in the
 219 observed patterns of forelimb and hind limb toepad surface area (see Supplemental Material).



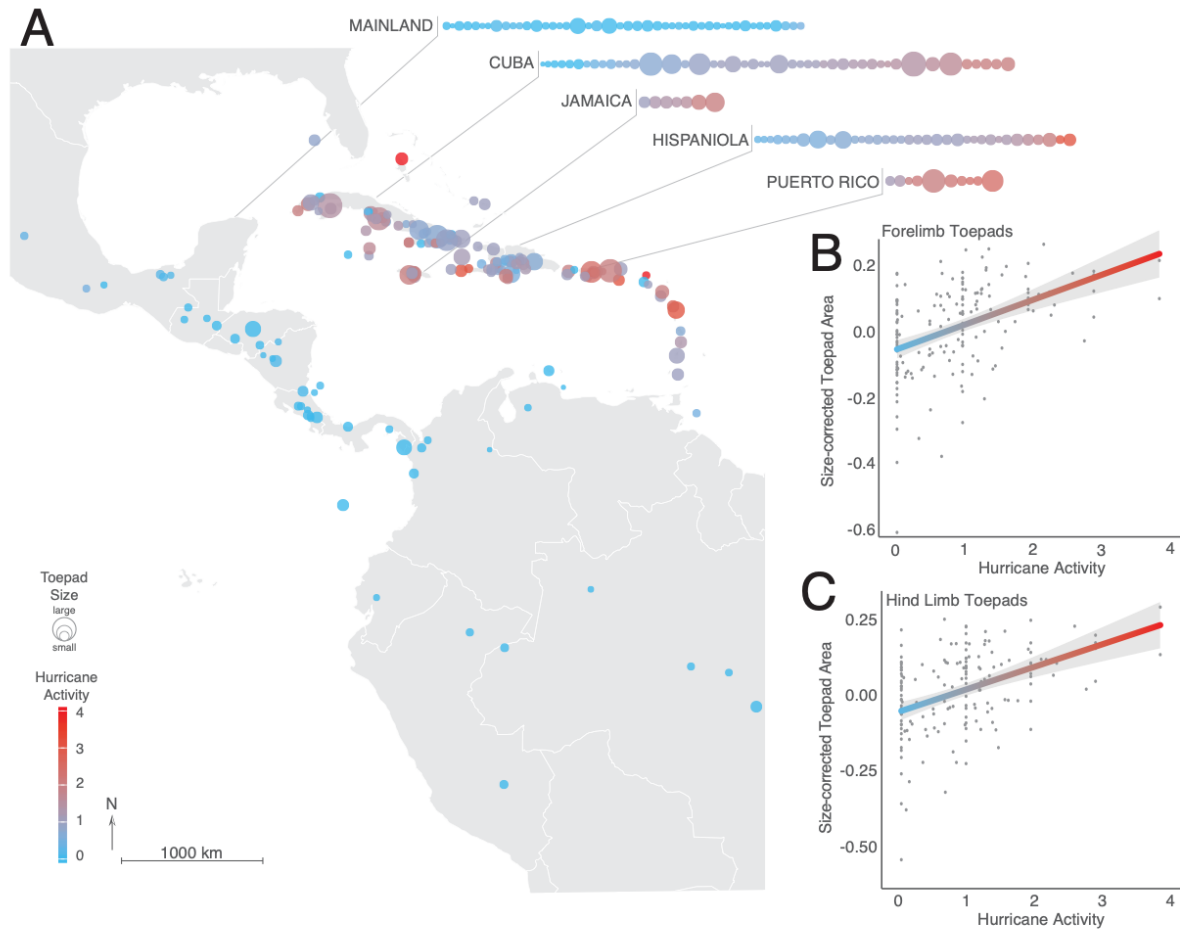
221
222

Fig 1. *Anolis scriptus*, like other anoles, use specialized toepads to cling to surfaces (D: inset images: a lizard clings to a perch while experiencing hurricane-force winds in a performance experiment, see 3). Populations of *A. scriptus* on Pine and Water Cays in the Turks and Caicos Islands (C) that survived 2017’s Hurricanes Irma and Maria had relatively larger toepads on average than the populations surveyed before the storms (3). When we resurveyed the populations in 2019 (A and B) following the storms, those body-size-corrected differences in toepad area persisted.

228



229
 230 **Fig 2.** By measuring toepad areas of individuals from 12 populations of *A. sagrei* (A), we found
 231 that populations that experienced more hurricanes in the last 70 years (red) had larger toepads
 232 than those that were hit less often (blue). In the map, each point corresponds to an island
 233 population, the size of the point corresponds to the relative toepad surface area of that
 234 population, and the color to the number of hurricanes experienced in the last 70 years.
 235 Regressions are of phylogenetically and body-size-corrected toepad area residuals for forelimbs
 236 (B) and hind limbs (C). See Supplemental Information for additional detail about the hurricane
 237 activity calculation.



238

239 **Fig 3.** Across the full geographic expanse of the *Anolis* clade, here with each point representing

240 one of 188 species, toepad area – accounting for phylogeny and body size – is significantly

241 positively correlated with the number of hurricanes experienced by that species over the last 70

242 years. (A) Each point represents the centroid of a species range, the color of that point indicates

243 the mean number of hurricanes experienced across the species' range, and the size of the point

244 corresponds to the average body-size-corrected toepad area. For clarity, we highlighted the

245 species on the mainland and on each of the Greater Antillean islands in callouts and ordered

246 them by increasing hurricane activity. Size-corrected residuals of forelimb (B) and hind limb (C)

247 toepad areas are positively related to hurricane activity.

248 **Methods:**

249 No statistical methods were used to pre-determine sample sizes for any aspect of this study.

250

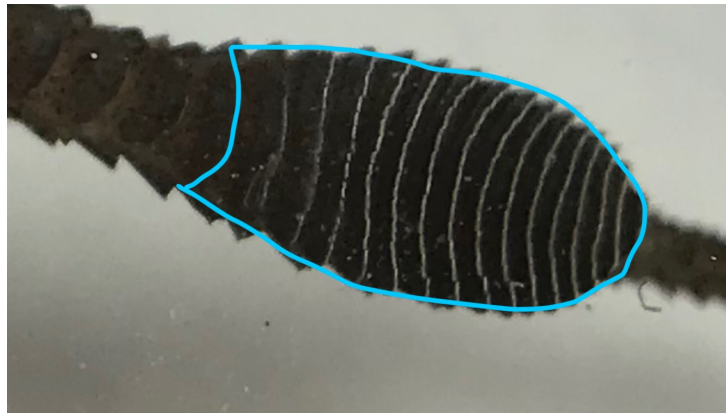
251 ***Anolis scriptus* in Turks and Caicos**

252 Pine Cay and Water Cay – two small islands in the Turks and Caicos Islands – are home
253 to the endemic Turks and Caicos anole, *Anolis s. scriptus*. Both islands are relatively small (Pine
254 Cay: 350 ha; Water Cay: 250 ha), flat, and covered by vegetation that averages between one and
255 three meters in height. Adult Turks and Caicos anoles range in size between 40 – 65 mm in
256 snout-to-vent length (SVL) and are sexually dimorphic: adult females are smaller than males.
257 The species is conspicuous and abundant and can typically be found perched on small branches
258 in the lower 1.5 m of the islands' vegetation (19).

259 Between 28 August and 4 September 2017, we surveyed the *A. scriptus* populations on
260 Pine Cay and Water Cay to establish baselines for the populations in anticipation of a
261 conservation project. Following a direct hit by Hurricane Irma (8 September 2017) and glancing
262 blow by Hurricane Maria (22 September 2017), we revisited the islands between 16 October and
263 20 October 2017 to determine whether the surviving lizard populations differed significantly in
264 morphology from the pre-hurricane populations (detailed in 3).

265 We repeated those surveys 18 months (1 April to 8 April 2019) after our initial post-
266 hurricane survey. For those revisits, the same researchers (CMD, A-CF, AH) walked the same,
267 approximately two-km-long transect on each island and caught lizards by hand or with a pole
268 and fishing line slipknot (following 3). In this way, we caught 117 lizards in 2019 (See Table
269 S1.1).

270 We repeated the morphological measurements from the pre- and post-hurricane sampling
271 for those lizards caught in 2018 and 2019. In brief, the same researcher (AH) measured
272 morphology using digital calipers (Mitutoyo 500-752), and CMD took a high-resolution
273 photograph of the right fore- and hind feet of each lizard using an iPhone 7 with a Moment
274 Macro Lens attachment (See 3 for additional details). Using ImageJ (v.1.51a., W. Rasband,
275 National Institute of Health, Bethesda), CMD measured the toepad area of the longest toe (digit
276 III on forelimb, digit IV on hind limb) on each lizard's right forelimb and hind limb to the first
277 scale after the toepad begins to widen (Fig. M1).



278
279 Fig. M1: An illustration of the toepad surface area measurement used for this study.

280
281 *Identifying lizards hatched since the 2017 hurricanes*

282 In order to determine whether the hurricanes had a sustained impact on the subsequent
283 generation of *A. scriptus* on Pine Cay and Water Cay, we calculated an estimate for how large a
284 lizard that hatched one year before the 2019 survey (and thus, necessarily the offspring of
285 hurricane survivors) might have grown. We used a logistic-by-length model that previous
286 researchers have demonstrated adequately characterizes growth for small-bodied anoles that are
287 ecologically similar to *A. scriptus* (20–22).

288

$$L_2 = \frac{\alpha L_1}{L_1 + (\alpha - L_1)e^{-rD}}$$

289
290 This model estimates final estimated body size (L_2) based upon initial size (L_1), time elapsed
291 (D), characteristic growth rates for the population (r) and the asymptotic maximum size (α). For
292 initial size we used 19 mm, an average hatchling size for *A. sagrei* (23). We parameterized D as
293 365 days, signifying an April 1, 2018 hatch date. We used separate values of α for males and
294 females using the largest *A. scriptus* individual of each sex we measured in any survey (male
295 maximum SVL: 65.75 mm in 2019 sample; female maximum SVL: 49.74 mm in 2017, post-
296 hurricane sample). As characteristic growth rate estimates have never been calculated for *A.*
297 *scriptus*, we identified studies that have previously calculated growth rates in ecologically
298 similar species (*A. sagrei*: 20, 22, *A. acutus*: 21). For our primary analysis, we used the lowest,
299 most conservative growth rates (male = 0.006, 21, and female = 0.0083, 22). Andrews'
300 calculated female growth rate was 0.009 resulting in a slightly larger, less conservative, female
301 body size estimate (Table S1.2). We re-analyzed the data using other growth rates and found the
302 same results (Appendix 1). Using these parameters, we calculated the maximum size of an
303 individual hatched on or after April 1, 2018 would be 46.13 mm for females and 51.55 mm for
304 males during our 2019 survey. April 1, 2018 was chosen as the earliest included hatch date
305 because lizards hatched earlier may have been derived from eggs that survived the hurricanes,
306 even if their parents did not, or could be the result of sperm storage from a male who did not
307 survive. We used these as cutoffs and analyzed all smaller lizards caught in 2019, assuming that
308 these lizards had hatched within the previous year (Table S1.3). See Appendix 1 for additional
309 data and details.

310 *Data analysis*

311 Our primary aim was to determine whether the toepads of the *A. scriptus* surveyed in
312 2019 were statistically different from those measured in 2017, either before or after the

313 hurricanes. To do so we used general linear models (GLM) with the surface area of the forelimb
314 toepads, or hind limb toepads as the response variable. We included body size – SVL – as a
315 factor in the GLM to account for differences in body size between the sampling times. In
316 addition, we added a factor for island of origin – Pine Cay or Water Cay – and an additional
317 fixed effect for each of the three sampling periods: pre-hurricane, post-hurricane, and 2019. Both
318 SVL and the toepad surface areas were log₁₀ transformed to improve normality of the data. See
319 Appendix 1 for complete model description. To evaluate differences between survey years, we
320 used the ‘lsmeans’ (24) and ‘effects’ (25, 26), packages in R (R Core Team). We used the same
321 analytical methods with the subset of lizards caught in 2019 and most likely having hatched
322 within the previous year.

323

324 **Comparative analyses among anole populations and species**

325 *Identifying lizard localities:*

326 *Anolis sagrei* is a common and widespread anole and is ecologically similar to *A. scriptus*
327 (8). It can be found on numerous islands in the West Indies, including the Bahamas, Cuba,
328 Jamaica, and the Caymans. As part of an ongoing comparative study on *A. sagrei* across its
329 range, CMD, AJG, and RGR collected data on individuals from 12 islands. All of these lizards
330 were captured in similar closed-canopy coppice forest in 2016 and 2017. We recorded the GPS
331 locations of these sampling sites during the collection surveys.

332 Locality data for the entire genus were drawn from a dataset published by Velasco et al.
333 (27). These locality data were collected from multiple sources including the Global Biodiversity
334 Information Facility (GBIF, <http://gbif.org>), HerpNet (<http://herpnet.org>) and previously
335 published distribution datasets (see 27 for complete list of sources).

336

337 *Calculating a hurricane activity measure*

338 We used each of the lizard locality points – for field-caught *A. sagrei* and the Velasco et
339 al. (27) records for the genus as a whole – to calculate the average number of hurricane hits for
340 each species.

341 We first obtained the latitude-longitude position and maximum sustained wind speed for
342 all tropical cyclones in the North Atlantic and eastern North Pacific basins between 1949 and
343 2017. Data from 1949 to 2016 were obtained from the International Best Track Archive for
344 Climate Stewardship v03r10 (IBTrACS; 28). Because 2017 IBTrACS data were not yet
345 available, we obtained the 2017 data from the Tropical Cyclone Extended Best Track dataset
346 (EBT; 29). Both of these datasets provide position and maximum sustained wind speed data for
347 each tropical cyclone every six hours at 0000, 0600, 1200, and 1800 UTC. IBTrACS also
348 provides data for some storms at intermediate times such as landfall events. Because 2017 EBT
349 data did not include these intermediate times, we added them using National Hurricane Center
350 storm reports (30) to ensure consistency across the dataset.

351 After all tropical cyclone data were compiled, we interpolated the storm position and
352 wind speed to 24 evenly spaced time intervals between each available data point. These
353 interpolated points provide an estimate of each tropical cyclone’s position and intensity every 15
354 minutes, or occasionally somewhat more frequently when intermediate time points (e.g., landfall
355 time) are also recorded. We interpolated both position and windspeed to ensure a hit was
356 counted: fast-moving storms may hit a population within the 6-hour window and yet exceed the
357 distance threshold at the six-hour increment, and had we not interpolated, they would not have
358 been counted.

359 For each of the anole locality points, we counted the number of tropical cyclones that
360 passed within a radius (30, 50, or 100 km), while meeting or exceeding a windspeed intensity
361 threshold (65, 80, 100 kt sustained winds; [1 kt = 0.514 ms⁻¹]) during the 1949-2017 period. We
362 specified in our counting algorithm that each tropical cyclone could only produce a single hit at
363 each GPS location, regardless of the number of time steps at which it satisfied the specified
364 distance and intensity criteria, or whether the storm reversed direction and hit a locality a second
365 time. We used MATLAB to calculate these hurricane counts (The MathWorks Inc., 2019;
366 Appendix 8). Using these data, we then calculated the mean hurricane hits for each species by
367 averaging the hurricane counts for each locality recorded for each species. This resulted in a
368 continuous hurricane activity measure. For our main analyses, we focused on strong hurricanes
369 reaching or exceeding 80 knots of sustained wind speed (see Appendix 6 for additional
370 thresholds), as we previously found in laboratory conditions that *A. scriptus* lizards were, on
371 average, blown off perches at 74.3 ± 2.3 knots (3). We also focused on direct hits, within 30 km
372 of a GPS point in the spatial database. We conducted a sensitivity analysis to investigate how
373 different windspeeds and radii thresholds affected our models (Appendix 6). In general, we
374 found that increasing the threshold radius decreased the explanatory power for our model, *ergo*
375 very distant hurricanes did not substantially affect populations. We also found that more
376 powerful hurricanes (windspeed reaching or exceeding 100 kts) had a stronger effect than
377 weaker storms (Appendix 6).

378 A consideration inherent to this dataset is that longer-term hurricane frequency at each
379 location almost certainly differs from the frequency during the seven-decade dataset available for
380 study (1949-2017). Direct strikes from hurricanes, especially strong hurricanes, are infrequent
381 events; thus, it is likely that some vulnerable locations did not experience any direct strikes

382 during this seven-decade window, even though they have experienced hurricanes on longer
383 timescales.

384 Beyond the infrequent, stochastic nature of hurricane strikes, hurricane activity
385 throughout the North Atlantic basin varies on time scales that are not well-reflected in this seven-
386 decade dataset. Atlantic hurricane activity is modulated on multidecadal scales by the Atlantic
387 Multidecadal Oscillation (AMO; 31), which affects North Atlantic sea-surface temperatures and
388 sea-level pressures. Positive (warm) AMO phases are associated with more numerous and
389 intense North Atlantic hurricanes (32). The interval covered in this study spans 44 years of
390 positive AMO (1949-1969; 1995-2017) and 25 years of negative AMO (1970-1994).

391 Research on prehistoric hurricanes has also revealed that North Atlantic hurricane
392 activity has also varied across much longer timescales. Using both sedimentary records and a
393 statistical model based on past climate reconstructions, Mann et al. (33) found a period of
394 enhanced North Atlantic hurricane activity approximately 1000 years Before Present (BP), with
395 a relatively quiescent period following it. Paleotempestological records also indicate low-
396 frequency variations in the locations impacted by hurricanes. Liu and Fearn (34) showed that
397 catastrophic hurricane strikes in northwest Florida were three to five times more frequent
398 between 3400-1000 years BP, compared to 5000-3400 years and 1000-0 years BP. Elsner et al.
399 (35) concluded that variations in the position and strength of the Bermuda High, associated with
400 the North Atlantic Oscillation, affected hurricane tracks and thus the regions impacted by
401 hurricanes. They found that periods of enhanced Gulf of Mexico hurricane activity coincided
402 with suppressed activity on the United States northeast coast on several time scales. Similarly,
403 McCloskey and Liu (36) found that periods of higher hurricane frequency in Nicaragua showed
404 lower hurricane frequency in the northern Caribbean and North American Atlantic coast,

405 whereas Baldini et al. (37) concluded that North Atlantic hurricane tracks have gradually shifted
406 northward during the last five centuries from natural, and more recently, anthropogenic
407 processes. Therefore, we do not assume that hurricane frequency at a point in the North Atlantic
408 basin during the 1949-2017 period is necessarily representative of hurricane frequency at that
409 location on longer time scales.

410

411 *Calculating mean tree heights*

412 Using the same locality database employed in calculating the number of hurricanes for
413 each species, we calculated the mean height of trees at that location using a tree heights dataset
414 published by Simard et al. in which they used 2005 satellite-based lidar to estimate global tree
415 heights (38). We calculated mean tree heights within a 30, 50, and 100 km radius of each
416 locality. The radii were chosen to match the radii of the hurricane activity algorithm. We then
417 averaged these tree heights for each radius and each locality to calculate a mean tree height for
418 every species in the database.

419

420 *Measuring toepads*

421 Toepad images of 10 *A. sagrei* individuals per island population were collected in the
422 field by RGR, AJG, and CMD and from museum specimens of all other species by DLM, HKF
423 and assistants using a flatbed scanner (Epson Perfection V500 Photo or Canon CanoScan LiDE
424 70). The preserved *Anolis* specimens used for this study are from the collections of the Harvard
425 Museum of Comparative Zoology, Field Museum of Natural History, Institute of Ecology and
426 Systematics (Havana, Cuba), and Drs. Steven Poe and Richard Glor. For all species in the
427 interspecific dataset, CMD measured toepad surface area (ImageJ) of the third toe on the

428 forelimb and the fourth (longest) toe on the hind limb following the same methods as the *A.*
429 *sagrei* and *A. scriptus* analyses (Fig. M1). Three adult individuals were measured for each of 175
430 species, and those measurements were averaged to calculate a species mean. For five additional
431 species, only two specimens were available, and eight species in the dataset had only one
432 available specimen. While these species with fewer than three specimens were included in the
433 published results, repeating the analysis with only those subsets of species with exactly three
434 specimens yielded similar significant results. Because mismatches between a species' average
435 toepad characteristics as estimated from our sample, and the average hurricanes experienced by
436 that species were potentially systematically exacerbated for wide-spread species, we repeated the
437 whole-genus analysis without the seven most widespread species (Appendix 7). We found the
438 same significant results.

439

440 ***Data analysis***

441 *Phylogenetic methods*

442 The phylogeny of *Anolis sagrei* populations (Fig. S2.1) was generated by pruning a larger
443 tree previously inferred by van de Schoot (39). Briefly, the mitochondrial-encoded locus
444 NADPH Dehydrogenase Subunit 2 (plus some post-terminal tRNA-encoding sequence) was
445 amplified and sequenced for specimens of *Anolis sagrei* from across the species' natural range.
446 Contig assembly and manual alignment was performed using Geneious R9.1
447 (<https://www.geneious.com>). The optimal partitioning scheme, and the model of molecular
448 evolution best fitting each partition was determined using PartitionFinder v1.1.1 (40). van de
449 Schoot used Bayesian Inference to estimate the phylogeny of this group using MrBayes v3.2.6
450 (41) and found all of the islands included in our sample to be monophyletic; therefore, for the

451 present study we pruned the phylogeny down to a single individual per island. For most islands
452 the individual used for the pruned phylogeny was a lizard for which we had also collected
453 morphological data. To represent the remaining islands (Eleuthera, South Bimini, Cay Sal,
454 Cayman Brac) in the phylogeny, we selected an individual collected from the same site and at
455 the same time as the lizards that were measured. For the phylogenetic comparative analyses
456 spanning the entire genus, we used a recent tree by Poe et al (42).

457 To account for phylogenetic non-independence in our comparative datasets, either
458 between the 12 *A. sagrei* populations or across the genus as a whole, we used phylogenetic
459 comparative linear models evaluated using the phytools (43), caper (44), GEIGER (45), ape (46),
460 and picante (47) packages in R (R core team).

461 Our phylogenetic generalized least squares models took the form:

$$462 \log_{10}(\text{toepad area}) \sim \log_{10}(\text{SVL}) + \text{Hurricane Activity}$$

463 with delta, and kappa transformations set to 1 and the lambda phylogenetic signal parameter
464 freely estimated (“ML”).

465

466 *Spatial Autocorrelation*

467 For the *A. sagrei* and genus-wide analyses, we tested whether phylogenetic regression
468 results were potentially influenced by residual spatial autocorrelation by constructing Moran’s I
469 correlograms. We calculated Moran’s I using 25km lag distances, e.g. all points separated by less
470 than 25km (in any direction), then points between 25km and 50km apart, and so on to a
471 maximum of 600km. We tested for significance using randomization tests. Correlograms were
472 generated using the correlog() function in the ncf package (48). We found no significant spatial
473 autocorrelation in residuals of any regression model at any lag distance ($P > 0.10$ in all cases),

474 suggesting that phylogenetic autocorrelation and hurricane activity can account for spatial
475 patterns in toepads and regression results are not confounded by spatial autocorrelation. Thus, we
476 did not consider spatial autocorrelation further (Fig. S2.2; S3.1, S3.6).

477

478 **Methods References:**

- 479 19. A. L. Laska, The structural niche of *Anolis scriptus* on Inagua. *Breviora* 349, 1-6 (1970).
- 480 20. T. W. Schoener, A. Schoener, Estimating and interpreting body-size growth in some *Anolis*
481 lizards. *Copeia* 3, 390–405 (1978).
- 482 21. R. B. Andrews, “Patterns of growth in reptiles” in: *Biology of the Reptilia*, C. Gans, F. H.
483 Pough, Eds. (Academic Press 1982), vol. 13, pp. 273–320.
- 484 22. A. N. Wright, J. Piovia-Scott, D. A. Spiller, G. Takimoto, L. H. Yang, T. W. Schoener,
485 Pulses of marine subsidies amplify reproductive potential of lizards by increasing individual
486 growth rate. *Oikos* 122: 1496-1504 (2013).
- 487 23. P. R. Pearson, D. A. Warner, Early hatching enhances survival despite beneficial phenotypic
488 effects of late-season developmental environments. *Proc. R. Soc. B.* 285, 20180256 (2018).
- 489 24. R. V. Lenth, Least-squares means: The R package lsmeans. *J of Stat. Softw.* 69, 1-33 (2016).
- 490 25. J. Fox, Effect displays in R for generalised linear models. *J. Stat. Softw.* 8, 1-27 (2003).
- 491 26. J. Fox, S. Weisberg, *An R companion to applied regression, 3rd edition* (Sage Publications,
492 Thousand Oaks, CA, 2019).
- 493 27. J. A. Velasco, F. Villalobos, J. A. F. Diniz-Filho, S. Poe, O. Flores-Villela, Macroecology
494 and macroevolution of body size in *Anolis* lizards. *Ecography* (2020).
- 495 28. National Centers for Environmental Information (NCEI), last accessed – 25 April 2019.
496 International Best Track Archive for Climate Stewardship (IBTrACS). Available online at
497 <https://www.ncdc.noaa.gov/ibtracs/index.php?name=ibtracs-data>.
- 498 29. Regional and Mesoscale Meteorology Branch (RAMMB), last accessed – 25 April 2019. The
499 Tropical Cyclone Extended Best Track Dataset. Available online at
500 http://rammb.cira.colostate.edu/research/tropical_cyclones/tc_extended_best_track_dataset/.
- 501 30. National Hurricane Center (NHC), last accessed – 25 April 2019. 2017 Atlantic Hurricane
502 Season. Available online at <https://www.nhc.noaa.gov/data/tcr/index.php?season=2017>
- 503 31. R. A. Kerr, A North Atlantic climate pacemaker for the centuries. *Science* 288, 1984-1985
504 (2000).
- 505 32. P. J. Klotzbach, W. M. Gray, Multidecadal variability in North Atlantic tropical cyclone
506 activity. *J. Climate* 21, 3929-3935 (2008).
- 507 33. M. E. Mann, J. D. Woodruff, J. P. Donnelly, Z. Zhang, Atlantic hurricanes and climate over
508 the past 1,500 years. *Nature* 460, 880-883 (2009).

- 509 34. K. Liu, M. L. Fearn, Reconstruction of prehistoric landfall frequencies of catastrophic
510 hurricanes in Northwestern Florida from lake sediment records. *Quaternary Res.* 54, 238-245
511 (2000).
- 512 35. J. B. Elsner, K. Liu, B. Kocher, Spatial variations in major U.S. hurricane activity: statistics
513 and a physical mechanism. *J. Climate* 13, 2293-2305 (2000).
- 514 36. T. A. McCloskey, K. Liu, A sedimentary-based history of hurricane strikes on the southern
515 Caribbean coast of Nicaragua. *Quaternary Res.* 78, 454-464 (2012).
- 516 37. L. M. Baldini, J. U. L. Baldini, J. N. McElwaine, A. Benoit Frappier, Y. Asmerom, K. Liu,
517 K. M. Prufer, H. E. Ridley, V. Polyak, D. J. Kennett, C. G. Macpherson, V. V. Aquino, J.
518 Awe, S. F. M. Breitenbach, Persistent northward North Atlantic tropical cyclone track
519 migration over the past five centuries. *Sci. Rep.* 6, 37522 (2016).
- 520 38. M. Simard, N. Pinto, J.B. Fisher, A. Baccini. Mapping Forest Canopy Height Globally with
521 Spaceborne Lidar. *Journal of Geophysical Research* 116 (2011).
- 522 39. M. van de Schoot, Within and between island radiation and genetic variation in *Anolis sagrei*
523 MSc Thesis, Wageningen University, Netherlands (2016).
- 524 40. R. Lanfear, B. Calcott, S. Y. Ho, S. Guindon, PartitionFinder: combined selection of
525 partitioning schemes and substitution models for phylogenetic analyses. *Molecular Biology*
526 *and Evolution*, 29, 1695-1701 (2012).
- 527 41. F. Ronquist, M. Teslenko, P. Van Der Mark, D. L. Ayres, A. Darling, S. Höhna, B. Larget, L.
528 Liu, M. A. Suchard, J. P. Huelsenbeck, MrBayes 3.2: efficient Bayesian phylogenetic
529 inference and model choice across a large model space. *Systematic Biology*, 61, 539-542
530 (2012).
- 531 42. S. Poe, A. Nieto-Montes de Oca, O. Torres-Carvajal, K. de Queiroz, J. A. Velasco, B. Truett,
532 L. N. Grey, M. J. Ryan, G. Köhler, F. Ayala-Varela, I. Latella, A phylogenetic,
533 biogeographic, and taxonomic study of all extant species of *Anolis* (Squamata; Iguanidae).
534 *Syst. Biol.* 66, 663-697 (2017).
- 535 43. L. J. Revell, phytools: An R package for phylogenetic comparative biology (and other
536 things). *Methods Ecol. Evol.* 3, 217-223 (2012).
- 537 44. D. Orme, R. Freckleton, G. Thomas, T. Petzoldt, S. Fritz, N. Isaac, W. Pearse, CAPER:
538 comparative analyses of phylogenetics and evolution in R. R package version 1.0.1.
539 <https://CRAN.R-project.org/package=caper> (2018).
- 540 45. L. J. Harmon, J. T. Weir, C. D. Brock, R. E. Glor, W. Challenger, GEIGER: investigating
541 evolutionary radiations. *Bioinformatics* 24, 129-131 (2008).
- 542 46. E. Paradis, K. Schliep, ape 5.0: an environment for modern phylogenetics and evolutionary
543 analyses in R. *Bioinformatics* 35, 526-528 (2018).
- 544 47. S. W. Kembel, P. D. Cowan, M. R. Helmus, W. K. Cornwell, H. Morlon, D. D. Ackerly, S.
545 P. Blomberg, C. O. Webb, Picante: R tools for integrating phylogenies and ecology.
546 *Bioinformatics* 26, 1463-1464 (2010).
- 547 48. O. N. Bjornstad, NCF: spatial covariance functions. R package version 1.2-8, (2019).

548 **Acknowledgements:**

549 This work was made possible thanks to the Pine Cay Homeowners Association with fieldwork
550 and logistical support from C. Santoro and E. Bell. We also thank E. Salamanca at the TCI
551 DECR. This research was approved by the Turks and Caicos DECR (Permit 19-03-04-10),
552 Bahamas Environment, Science, and Technology Commission (2015, 2016, 2017), Cayman DoE
553 (2015-ACSS078), and Harvard IACUC (26-11).

554

555 **Funding:**

556 NSF – IOS-1354620 to JBL & AH; NSF – RAPID ISO-1806420 to JJK & JBL; NSF –
557 Postdoctoral Fellowship #1609284 to CMD; NSF – DDIG DEB #1500761 to AJG; Harvard
558 MCZ Putnam Expedition Grant to RGR; FWO Postdoctoral Fellowship #12I8819N to SB;
559 DGAPA-UNAM Postdoctoral Fellowship to JAV. In addition, this publication was made
560 possible through the support of a grant from the John Templeton Foundation. The opinions
561 expressed in this publication are those of the author(s) and do not necessarily reflect the views of
562 the John Templeton Foundation.

563

564 **Author Contributions:**

565 CMD initiated the study; CMD, AH, and A-CF collected *A. scriptus* field data, CMD, AJG, and
566 RGR collected *A. sagrei* field data; additional datasets were contributed by AK (hurricane
567 activity), HKF, DLM with help from SB (*Anolis*-wide toepad photos), AA, JV (*Anolis*
568 distribution), AA (tree heights), and AJG (*A. sagrei* phylogeny); CMD, DLM, AA, and RWB

569 analyzed the data; CMD prepared figures; CMD, JTS, and JBL wrote the manuscript; all authors
570 contributed to improving the final manuscript draft.

571

572 **Competing Interests:** The authors declare no competing interests.

573

574 **Data and Materials Availability:** Upon publication, all data will be made available on the
575 DRYAD digital repository.

Supplementary Materials for:

Hurricane Effects on Neotropical Lizards Span Geographic and Phylogenetic Scales

Authors: C.M. Donihue, A. Kowaleski, J.B. Losos, A.C. Algar, S. Baeckens, R.W. Buchkowski, A.-C. Fabre, H.K. Frank, A.J. Geneva, R.G. Reynolds, J.T. Stroud, J.A. Velasco, J.J. Kolbe, D.L. Mahler, A. Herrel

Correspondence to: colindonihue@gmail.com

This PDF file includes:

Materials and Methods

Appendix 1: *Anolis scriptus*

Table S1.1 – S1.3

Appendix 2: *Anolis sagrei*

Fig. S2.1 – S2.2

Appendix 3: *Anolis* across its range

Fig S3.1- S3.6

Appendix 4: Tree Heights

Appendix 5: Bioclimatic Data

Figure S5.1 – S5.4

Appendix 6: Sensitivity Analysis

Figure S6.1 – S6.3

Appendix 7: Species sampling

Appendix 8: Matlab code for calculating hurricane strikes

Appendix 1: *Anolis scriptus*

Table S1.1: Number of *Anolis scriptus* on Pine Cay and Water Cay measured during the three surveys.

	Pine Cay		Water Cay	
	Female	Male	Female	Male
Pre-Hurricane, 2017	19	18	20	20
Post-Hurricane, 2017	24	29	28	25
2019	26	33	31	27

Table S1.2: Parameters used for estimating the logistic-by-length growth rate cut-offs for *A. scriptus* on Pine Cay and Water Cay that had most likely hatched within one year of the 2019 survey (and therefore parented by hurricane survivors). Three parameters were employed based upon our data and question (D , L_1 , α). A characteristic growth rate has never been calculated for *A. scriptus*, and so we instead used four published estimates for males and females of ecologically similar anoles (*A. sagrei*, *A. acutus*). Using these parameters, we calculated SVL estimates (see logistic-by-length equation in-text or 20). We then used the most conservative male and female SVL estimates to serve as our cutoff for subsequent analyses.

Growth Estimate Parameters					
$D =$	365	Time since hatching (days)			
$L_1 =$	19	Hatching size (mm)			
$\alpha =$	65.75	Male asymptote (mm)			
$\alpha =$	49.74	Female asymptote (mm)			
$r =$ (Published Growth Rates)					
	Male	Female	Species	notes	citation
$r_1 =$	0.0143	0.0116	<i>A. sagrei</i>		(20) Schoener & Schoener 1978
$r_2 =$	0.006	0.009	<i>A. acutus</i>		(21) Andrews 1976
$r_3 =$		0.0109	<i>A. sagrei</i>	Nutrient-Subsidized	(22) Wright et al. 2013
$r_4 =$		0.0083	<i>A. sagrei</i>	Nutrient-Unsubsidized	(22) Wright et al. 2013
SVL Estimates					
	Male	Female			
$r_1 =$	64.89	48.60			
$r_2 =$	51.55	46.90			
$r_3 =$	62.86	48.28			
$r_4 =$	58.76	46.13			

Table S1.3: The number of individuals on Pine Cay and Water Cay caught in 2019 that were smaller than the maximum body size estimated for a one-year-old individual based on the growth estimates calculated in Table S1.2. The conservative growth rate for males (r_2) led to a dramatic reduction in male sample size. The second most conservative threshold (r_4) led to a much higher inclusion rate in the dataset (2019*). The change in sample sizes, however, did not change the outcome of the results: the lizards measured in 2019 most likely to have had hurricane-survivor parents were statistically indistinguishable from the population measured immediately post-hurricane and were significantly different from those measured immediately before the hurricanes.

	Pine Cay		Water Cay	
	Female	Male	Female	Male
2019 (r_2)	25	4	30	5
2019* (r_4)	25	20	30	26

Supplemental Analysis 1.1:

The conservative SVL cutoff used in the manuscript (r_2) for males dramatically decreased sample sizes for the 2019 lizards (Table S1.3). As this was the lowest, most conservative relevant growth rate we found in the literature, we used it for the primary reported analyses in the manuscript. However, including only nine males between the two islands means that this analysis may be unduly skewed by outliers or atypical individuals. We thus repeated the analysis with the second most conservative growth rate (r_4). This growth estimate included more of the lizards measured in 2019 (Table S1.3) and a proportion of the male individuals that was more in-line with the proportion identified for females. The (r_4) rate for males was still substantially lower than two other growth rates in the literature, and in our opinion still represents a reasonable conservative estimate for the growth rate of *A. scriptus* in the year preceding the 2019 survey.

Regardless of the growth rate used, the analysis yielded the same results. The lizards measured in 2019 that had most likely hatched in the year preceding the survey were statistically indistinguishable from the lizards that survived the hurricanes and had significantly larger toepads than those measured before the hurricanes.

For all subsequent analyses our model took the form:

$$\log_{10}(\text{toepad area}) \sim \log_{10}(\text{SVL}) + \text{Hurricane} [\text{Before}|\text{After}|2018|2019] \\ + \text{Origin}[\text{Pine Cay}|\text{WaterCay}] + \text{Sex}[\text{Male}|\text{Female}]$$

Growth rate (r_2): Forelimb Toepads:

Coefficients:

	Estimate	Std. Error	t value	Pr(> t)	
(Intercept)	-8.21243	0.25007	-32.840	< 2e-16	***
log(SVL)	2.20223	0.06806	32.357	< 2e-16	***
HurricaneAfter	0.00597	0.01798	0.332	0.7401	
HurricaneBefore	-0.12409	0.02039	-6.086	4.01e-09	***
OriginWater Cay	0.03714	0.01396	2.660	0.0083	**
SexMale	0.09733	0.01875	5.192	4.13e-07	***

Signif. codes: 0 '***' 0.001 '**' 0.01 '*' 0.05 '.' 0.1 ' ' 1

Residual standard error: 0.1142 on 267 degrees of freedom
(5 observations deleted due to missingness)

Multiple R-squared: 0.9094, Adjusted R-squared: 0.9077

F-statistic: 536 on 5 and 267 DF, p-value: < 2.2e-16

contrast	estimate	SE	df	t.ratio	p.value
2019 - After	-0.00597	0.0180	267	-0.332	0.7401
2019 - Before	0.12409	0.0204	267	6.086	<.0001
After - Before	0.13006	0.0173	267	7.535	<.0001

Results are averaged over the levels of: Origin, Sex
Results are given on the log (not the response) scale.
P value adjustment: holm method for 3 tests

Anova Table (Type III tests)

Response: log(FingerArea)

	Sum Sq	Df	F value	Pr(>F)	
(Intercept)	14.0727	1	1078.4629	< 2.2e-16	***
log(SVL)	13.6620	1	1046.9871	< 2.2e-16	***
Hurricane	0.8094	2	31.0125	7.748e-13	***
Origin	0.0923	1	7.0733	0.008297	**
Sex	0.3517	1	26.9535	4.134e-07	***
Residuals	3.4840	267			

Signif. codes: 0 '***' 0.001 '**' 0.01 '*' 0.05 '.' 0.1 ' ' 1

Growth rate (r_4): Forelimb Toepads:

Coefficients:

	Estimate	Std. Error	t value	Pr(> t)
(Intercept)	-8.13035	0.22437	-36.237	< 2e-16 ***
log(SVL)	2.17945	0.06061	35.961	< 2e-16 ***
HurricaneAfter	0.01195	0.01498	0.798	0.42570
HurricaneBefore	-0.11722	0.01719	-6.818	4.97e-11 ***
OriginWater Cay	0.03531	0.01284	2.750	0.00633 **
SexMale	0.09830	0.01833	5.364	1.62e-07 ***

Signif. codes: 0 '***' 0.001 '**' 0.01 '*' 0.05 '.' 0.1 ' ' 1

Residual standard error: 0.112 on 304 degrees of freedom
(5 observations deleted due to missingness)
Multiple R-squared: 0.9173, Adjusted R-squared: 0.916
F-statistic: 674.7 on 5 and 304 DF, p-value: < 2.2e-16

contrast	estimate	SE	df	t.ratio	p.value
2019 - After	-0.0119	0.0150	304	-0.798	0.4257
2019 - Before	0.1172	0.0172	304	6.818	<.0001
After - Before	0.1292	0.0169	304	7.644	<.0001

Results are averaged over the levels of: Origin, Sex
Results are given on the log (not the response) scale.
P value adjustment: holm method for 3 tests

Anova Table (Type III tests)

Response: log(FingerArea)

	Sum Sq	Df	F value	Pr(>F)
(Intercept)	16.4824	1	1313.1265	< 2.2e-16 ***
log(SVL)	16.2318	1	1293.1633	< 2.2e-16 ***
Hurricane	0.8244	2	32.8399	1.223e-13 ***
Origin	0.0949	1	7.5599	0.006325 **
Sex	0.3611	1	28.7699	1.617e-07 ***
Residuals	3.8158	304		

Signif. codes: 0 '***' 0.001 '**' 0.01 '*' 0.05 '.' 0.1 ' ' 1

Growth rate (r_2): Hind Limb Toepads:

Coefficients:

	Estimate	Std. Error	t value	Pr(> t)	
(Intercept)	-7.92374	0.21839	-36.283	< 2e-16	***
log(SVL)	2.25173	0.05943	37.889	< 2e-16	***
HurricaneAfter	0.01118	0.01571	0.711	0.477	
HurricaneBefore	-0.09296	0.01772	-5.246	3.15e-07	***
OriginWater Cay	-0.01374	0.01222	-1.124	0.262	
SexMale	0.09603	0.01641	5.851	1.42e-08	***

Signif. codes: 0 '***' 0.001 '**' 0.01 '*' 0.05 '.' 0.1 ' ' 1

Residual standard error: 0.1003 on 269 degrees of freedom
(3 observations deleted due to missingness)

Multiple R-squared: 0.9327, Adjusted R-squared: 0.9314
F-statistic: 745.3 on 5 and 269 DF, p-value: < 2.2e-16

contrast	estimate	SE	df	t.ratio	p.value
2019 - After	-0.0112	0.0157	269	-0.711	0.4774
2019 - Before	0.0930	0.0177	269	5.246	<.0001
After - Before	0.1041	0.0151	269	6.905	<.0001

Results are averaged over the levels of: Origin, Sex
Results are given on the log (not the response) scale.
P value adjustment: holm method for 3 tests

Anova Table (Type III tests)

Response: log(ToeArea)

	Sum Sq	Df	F value	Pr(>F)	
(Intercept)	13.2476	1	1316.4639	< 2.2e-16	***
log(SVL)	14.4463	1	1435.5815	< 2.2e-16	***
Hurricane	0.5098	2	25.3305	8.335e-11	***
Origin	0.0127	1	1.2645	0.2618	
Sex	0.3445	1	34.2303	1.418e-08	***
Residuals	2.7070	269			

Signif. codes: 0 '***' 0.001 '**' 0.01 '*' 0.05 '.' 0.1 ' ' 1

Growth rate (r_4): Hind Limb Toepads:

Coefficients:

	Estimate	Std. Error	t value	Pr(> t)	
(Intercept)	-7.941659	0.200262	-39.656	< 2e-16	***
log(SVL)	2.255307	0.054103	41.685	< 2e-16	***
HurricaneAfter	0.010978	0.013412	0.819	0.414	
HurricaneBefore	-0.093615	0.015308	-6.115	2.95e-09	***
OriginWater Cay	-0.005056	0.011477	-0.441	0.660	
SexMale	0.096399	0.016351	5.896	9.88e-09	***

Signif. codes: 0 '***' 0.001 '**' 0.01 '*' 0.05 '.' 0.1 ' ' 1

Residual standard error: 0.1003 on 305 degrees of freedom
(4 observations deleted due to missingness)
Multiple R-squared: 0.9366, Adjusted R-squared: 0.9356
F-statistic: 901.7 on 5 and 305 DF, p-value: < 2.2e-16

contrast	estimate	SE	df	t.ratio	p.value
2019 - After	-0.0110	0.0134	305	-0.819	0.4137
2019 - Before	0.0936	0.0153	305	6.115	<.0001
After - Before	0.1046	0.0151	305	6.949	<.0001

Results are averaged over the levels of: Origin, Sex
Results are given on the log (not the response) scale.
P value adjustment: holm method for 3 tests

Anova Table (Type III tests)

Response: log(ToeArea)

	Sum Sq	Df	F value	Pr(>F)	
(Intercept)	15.8060	1	1572.6226	< 2.2e-16	***
log(SVL)	17.4646	1	1737.6464	< 2.2e-16	***
Hurricane	0.5418	2	26.9518	1.666e-11	***
Origin	0.0020	1	0.1941	0.6599	
Sex	0.3494	1	34.7600	9.881e-09	***
Residuals	3.0655	305			

Signif. codes: 0 '***' 0.001 '**' 0.01 '*' 0.05 '.' 0.1 ' ' 1

Appendix 2: *Anolis sagrei*

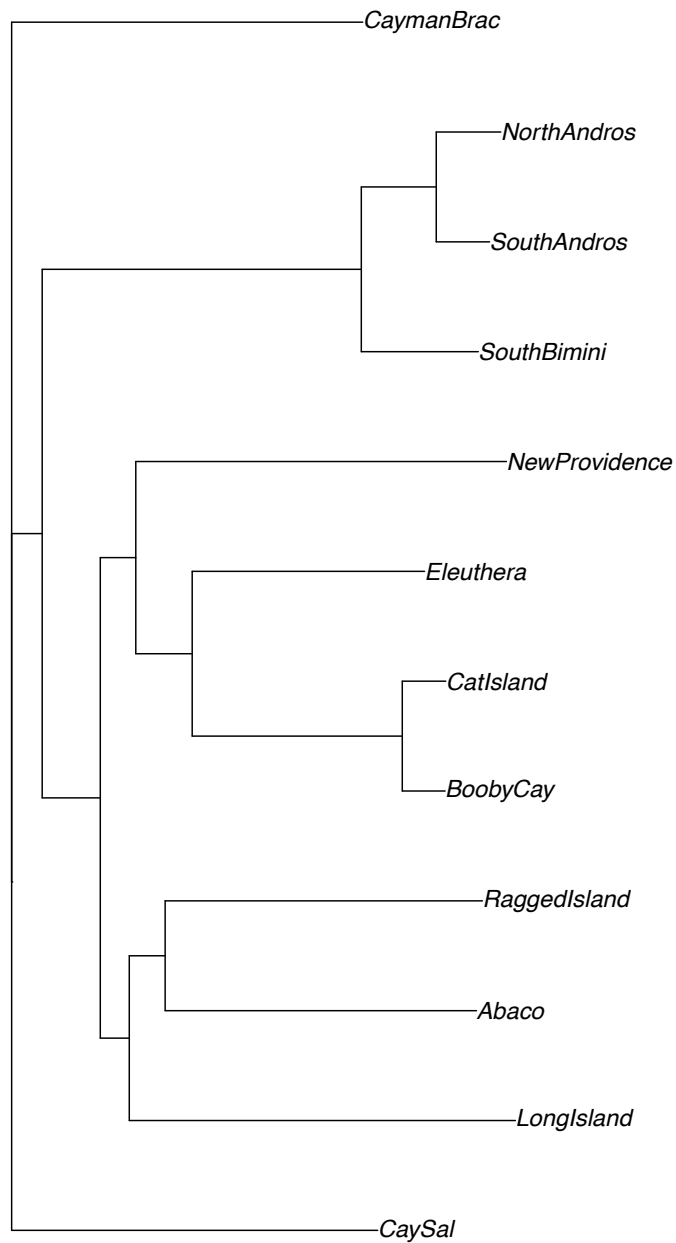


Fig. S2.1: The *A. sagrei* tree used for the phylogenetic comparative analyses. Branch ends are the island names where each population resides.

Forelimb Toepad Area:

Variable codes are:

fore_area: forelimb toepad area

log10svl: log-transformed body length

h80_30: number of hurricanes exceeding 80 knots of wind within 30 km of site

```
pgls(formula = log10(fore_area) ~ log10svl + h80_30, data = comp_sagrei_dat,
      lambda = "ML", kappa = 1, delta = 1, bounds = list(delta = c(1e-06,
      3)))
```

Residuals:

Min	1Q	Median	3Q	Max
-0.26757	-0.04259	0.09646	0.20087	0.34285

Branch length transformations:

```
kappa [Fix] : 1.000
lambda [ ML] : 0.000
  lower bound : 0.000, p = 1
  upper bound : 1.000, p = 0.035505
  95.0% CI    : (NA, 0.972)
delta [Fix] : 1.000
```

Coefficients:

	Estimate	Std. Error	t value	Pr(> t)	
(Intercept)	-3.622045	0.649606	-5.5758	0.0003448	***
log10svl	2.181836	0.389431	5.6026	0.0003332	***
h80_30	0.050485	0.017542	2.8780	0.0182381	*

```
---
Signif. codes:  0 '***' 0.001 '**' 0.01 '*' 0.05 '.' 0.1 ' ' 1
```

Residual standard error: 0.2123 on 9 degrees of freedom
Multiple R-squared: 0.8708, Adjusted R-squared: 0.842
F-statistic: 30.32 on 2 and 9 DF, p-value: 0.0001003

Hind Limb Toepad Area:

Variable codes are:

hind_area: hind limb toepad area

log10svl: log-transformed body length

h80_30: number of hurricanes exceeding 80 knots of wind within 30 km of site

The PGLS model with $\delta = 1$ fails to converge. Using ML to estimate δ and λ simultaneously suggests the following relationship:

```
ppls(formula = log10(hind_area) ~ log10svl + h80_30, data = comp_sagrei_dat,
      lambda = "ML", kappa = 1, delta = "ML", bounds = list(delta = c(1e-06,
3)))
```

Residuals:

	Min	1Q	Median	3Q	Max
	-0.08356	-0.02510	0.01249	0.05534	0.12437

Branch length transformations:

```
kappa [Fix] : 1.000
lambda [ ML] : 0.000
  lower bound : 0.000, p = 1
  upper bound : 1.000, p = 0.041964
  95.0% CI    : (NA, 0.982)
delta [ ML] : 0.304
  lower bound : 0.000, p = 3.956e-08
  upper bound : 3.000, p = 0.1186
  95.0% CI    : (0.008, NA)
```

Coefficients:

	Estimate	Std. Error	t value	Pr(> t)	
(Intercept)	-3.507083	0.527917	-6.6432	9.447e-05	***
log10svl	2.225089	0.317047	7.0182	6.199e-05	***
h80_30	0.055628	0.014333	3.8810	0.003725	**

Signif. codes: 0 '***' 0.001 '**' 0.01 '*' 0.05 '.' 0.1 ' ' 1

Residual standard error: 0.07283 on 9 degrees of freedom
Multiple R-squared: 0.9203, Adjusted R-squared: 0.9026
F-statistic: 51.97 on 2 and 9 DF, p-value: 1.139e-05

For in-text results, delta was parameterized as 0.3, lambda as ML.

```
pgls(formula = log10(hind_area) ~ log10svl + h80_30, data = comp_sagrei_dat,  
      lambda = "ML", kappa = 1, delta = 0.3, bounds = list(delta = c(1e-06,  
3)))
```

Residuals:

Min	1Q	Median	3Q	Max
-0.078264	-0.019476	-0.002275	0.061900	0.123725

Branch length transformations:

```
kappa [Fix] : 1.000  
lambda [ ML] : 0.000  
  lower bound : 0.000, p = 1  
  upper bound : 1.000, p = 0.041081  
  95.0% CI   : (NA, 0.980)  
delta [Fix] : 0.300
```

Coefficients:

	Estimate	Std. Error	t value	Pr(> t)
(Intercept)	-3.507257	0.527843	-6.6445	9.433e-05 ***
log10svl	2.225201	0.317000	7.0196	6.190e-05 ***
h80_30	0.055630	0.014332	3.8814	0.003723 **

```
---  
Signif. codes:  0 '***' 0.001 '**' 0.01 '*' 0.05 '.' 0.1 ' ' 1
```

```
Residual standard error: 0.07251 on 9 degrees of freedom  
Multiple R-squared: 0.9203, Adjusted R-squared: 0.9026  
F-statistic: 51.99 on 2 and 9 DF, p-value: 1.137e-05
```

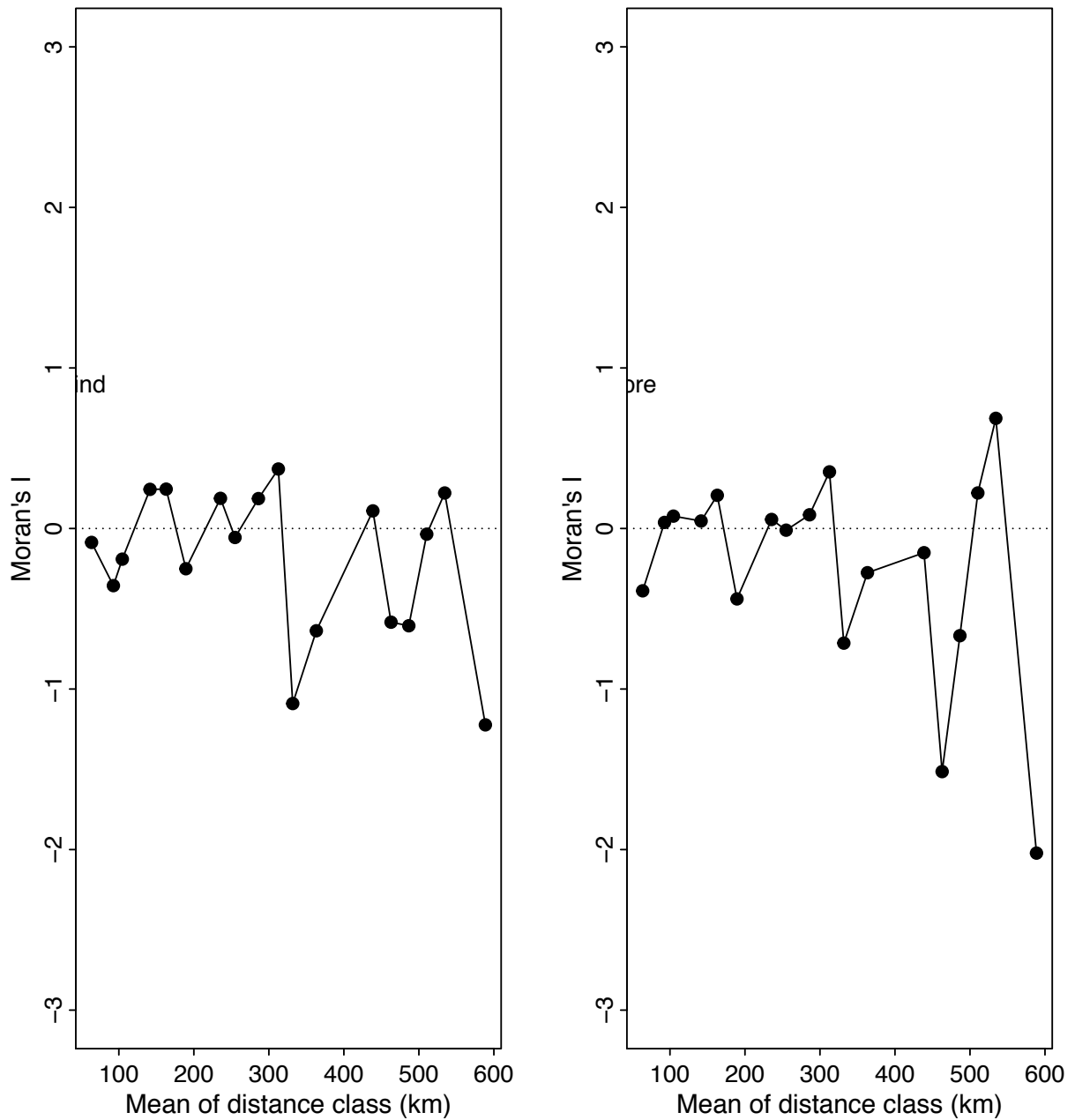


Fig. S2.2: Plot of Moran's I correlograms of hind limb toepad area (left) and forelimb toepad area (right) for 12 populations of *A. sagrei*. We found no structure in the residuals to indicate spatial autocorrelation in the data.

Appendix 2.2 Analyzing hurricane characteristics as a predictor of toepad area in *A. sagrei*

An open question is whether the time elapsed since the last hurricane or the strength of that hurricane affects the observed pattern in fore- and hind limb toepad area. We predicted, *a priori* that there might be a negative relationship between time since last hurricane and toepad areas – populations more recently hit by a hurricane would have relatively larger toepads whereas populations with a relatively longer elapsed time since the last hurricane strike might have proportionally smaller toepads. Moreover, we also predicted that populations experiencing a stronger recent hurricane would have relatively larger toepads than those experiencing a weaker hurricane at a similar time.

Due to gaps in collection dates and GPS localities in the cross-genus comparative analysis (Appendix 3) we are unable to satisfactorily address this question for the genus as a whole. Our *A. sagrei* collections, in contrast, have both high-resolution GPS coordinates and known collection times, and so are suited for a preliminary exploration of this question.

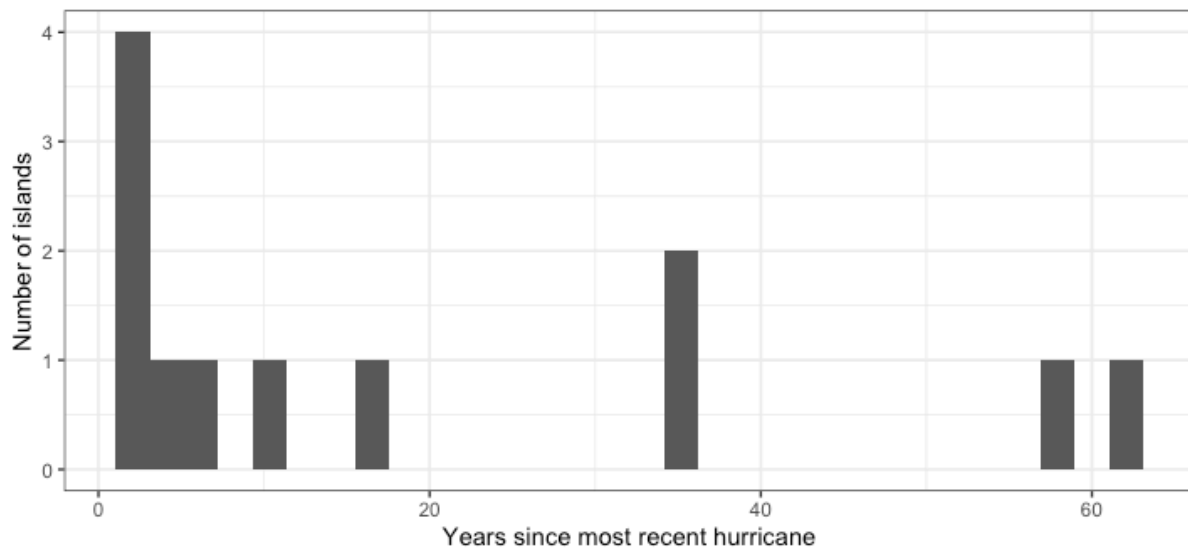


Figure 1 (above) shows the distribution of years since the last hurricane for the 12 Caribbean populations of *A. sagrei* used in this study. Eight of the island populations have had a direct hit by a tropical cyclone (within 30 km of the sampling area and by a storm exceeding 64 kts, the minimum windspeed threshold of NOAA’s database) within the last 20 years.

We then analyzed whether time since most recent hurricane predicted variation in toepad area across these twelve populations. We did not find a statistically significant relationship:

Forelimb toepad area:

log10(Forelimb Toepad Area) ~ log10(SVL) + Time_elapsed

Coefficients:

	Estimate	Std. Error	t value	Pr(> t)	
(Intercept)	-4.2042556	0.8730033	-4.816	0.000952	***
log10(SVL)	2.5868819	0.5083294	5.089	0.000655	***
Time_elapsed	-0.0006062	0.0011944	-0.507	0.624009	

Signif. codes: 0 '***' 0.001 '**' 0.01 '*' 0.05 '.' 0.1 ' ' 1

Residual standard error: 0.07983 on 9 degrees of freedom

Multiple R-squared: 0.7934, Adjusted R-squared: 0.7475

F-statistic: 17.29 on 2 and 9 DF, p-value: 0.0008272

Hindlimb toepad area:

log10(Hind Limb Toepad Area) ~ log10(SVL) + Time_elapsed

Coefficients:

	Estimate	Std. Error	t value	Pr(> t)	
(Intercept)	-4.0571486	0.8664043	-4.683	0.001148	**
log10(SVL)	2.6180992	0.5044870	5.190	0.000572	***
Time_elapsed	-0.000732	0.0011854	-0.618	0.551971	

Signif. codes: 0 '***' 0.001 '**' 0.01 '*' 0.05 '.' 0.1 ' ' 1

Residual standard error: 0.07923 on 9 degrees of freedom

Multiple R-squared: 0.8028, Adjusted R-squared: 0.7589

F-statistic: 18.32 on 2 and 9 DF, p-value: 0.0006721

In addition, we did not find a statistically significant relationship between the strength (windspeed at time of impact: "H1_VMAX") of the most recent hurricane and the relative size of the fore- or hind limb toepads.

Forelimb toepad area:

$\log_{10}(\text{Forelimb Toepad Area}) \sim \log_{10}(\text{SVL}) + \text{H1_VMAX}$

Coefficients:

	Estimate	Std. Error	t value	Pr(> t)	
(Intercept)	-4.103339	0.720896	-5.692	0.000297	***
$\log_{10}(\text{SVL})$	2.407560	0.447679	5.378	0.000446	***
H1_VMAX	0.002228	0.001375	1.621	0.139452	

Signif. codes: 0 '***' 0.001 '**' 0.01 '*' 0.05 '.' 0.1 ' ' 1

Residual standard error: 0.07123 on 9 degrees of freedom

Multiple R-squared: 0.8356, Adjusted R-squared: 0.799

F-statistic: 22.86 on 2 and 9 DF, p-value: 0.0002966

Hind limb toepad area:

$\log_{10}(\text{Hind Limb Toepad Area}) \sim \log_{10}(\text{SVL}) + \text{H1_VMAX}$

Coefficients:

	Estimate	Std. Error	t value	Pr(> t)	
(Intercept)	-4.074072	0.765698	-5.321	0.000481	***
$\log_{10}(\text{SVL})$	2.535630	0.475502	5.333	0.000473	***
H1_VMAX	0.001657	0.001460	1.135	0.285748	

Signif. codes: 0 '***' 0.001 '**' 0.01 '*' 0.05 '.' 0.1 ' ' 1

Residual standard error: 0.07566 on 9 degrees of freedom

Multiple R-squared: 0.8201, Adjusted R-squared: 0.7802

F-statistic: 20.52 on 2 and 9 DF, p-value: 0.0004438

This result can also be seen in the following figures:

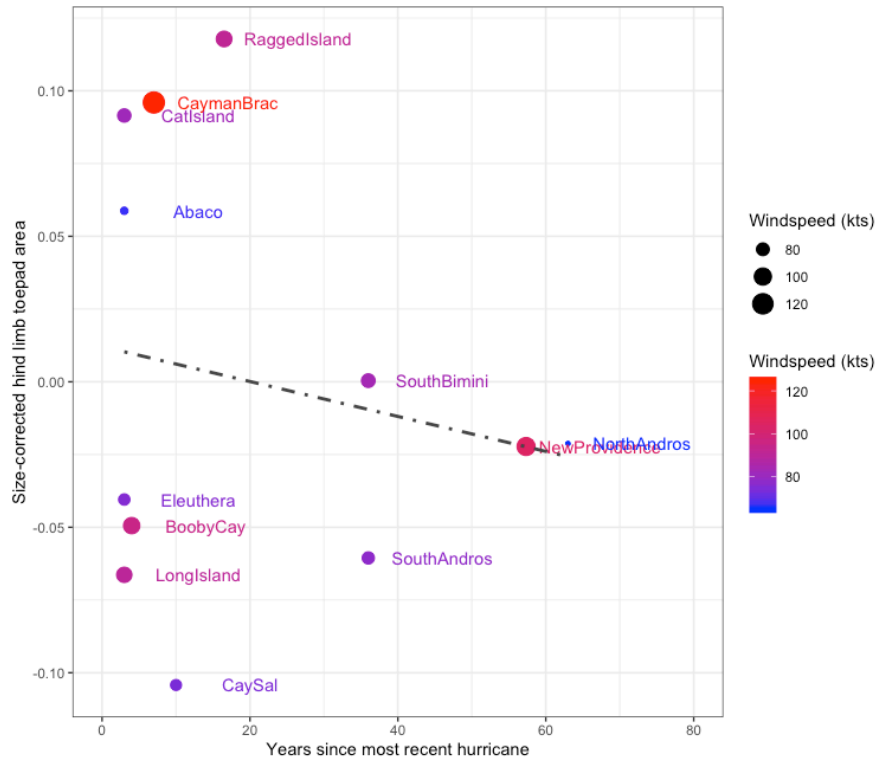
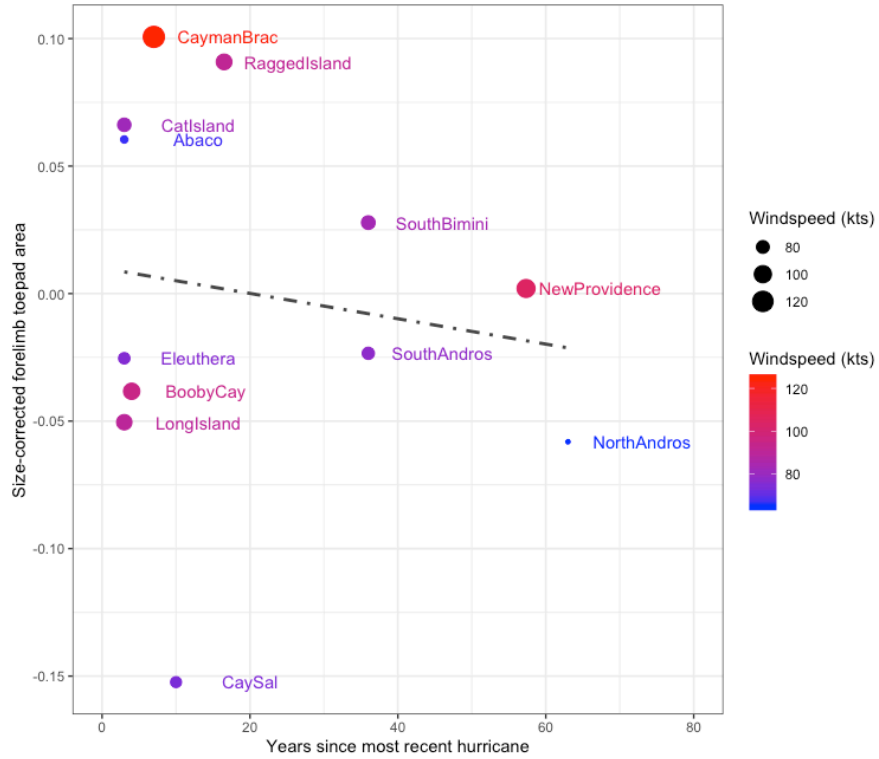


Figure 2 and 3: Relative forelimb and hind limb toepad area plotted against time elapsed since the most recent hurricane. Colors and size of the points correspond to the windspeed of the hurricane when it hit the study site (within 30 km). Dashed trend lines were added for illustration, though no statistically significant relationship was found.

This analysis implies no relationship between time since last hurricane and toepad area. One interpretation of this result is a slow relaxation of selection on toepads following the hurricanes. That said, this analysis would be substantially improved by repeated sampling within islands enabling a gradient of time-since-hurricane measurements. As of yet, we feel this result is preliminary and warrants further work to better understand the dynamics of the relaxation of selection following a hurricane.

Appendix 3: *Anolis* Across Its Range:

Appendix 3.1 The full *Anolis* radiation

Forelimb Toepad Area:

Variable codes are:

fore_area: forelimb toepad area

log10svl: log-transformed body length

h80_30: number of hurricanes exceeding 80 knots of wind within 30 km of site

```
pgls(formula = log10(fore_area) ~ log10svl + h80_30, data = comp_toepad_data,
      lambda = "ML", kappa = 1, delta = 1, bounds = list(delta = c(1e-06,
15)))
```

Residuals:

	Min	1Q	Median	3Q	Max
	-1.42270	-0.31776	-0.04874	0.31395	1.55929

Branch length transformations:

```
kappa [Fix] : 1.000
lambda [ ML] : 0.615
  lower bound : 0.000, p = 2.7845e-07
  upper bound : 1.000, p = 5.5511e-16
  95.0% CI   : (0.383, 0.794)
delta [Fix] : 1.000
```

Coefficients:

	Estimate	Std. Error	t value	Pr(> t)	
(Intercept)	-4.117143	0.128793	-31.9672	< 2.2e-16	***
log10svl	2.420760	0.070677	34.2509	< 2.2e-16	***
h80_30	0.060627	0.012050	5.0314	1.261e-06	***

```
---
Signif. codes:  0 '***' 0.001 '**' 0.01 '*' 0.05 '.' 0.1 ' ' 1
```

Residual standard error: 0.4916 on 165 degrees of freedom

Multiple R-squared: 0.8832, Adjusted R-squared: 0.8818

F-statistic: 623.9 on 2 and 165 DF, p-value: < 2.2e-16

Hind Limb Toepad Area:

Variable codes are:

hind_area: hind limb toepad area

log10svl: log-transformed body length

h80_30: number of hurricanes exceeding 80 knots of wind within 30 km of site

```
pgls(formula = log10(hind_area) ~ log10svl + h80_30, data = comp_toepad_data,
      lambda = "ML", kappa = 1, delta = 1, bounds = list(delta = c(1e-06,
      15)))
```

Residuals:

Min	1Q	Median	3Q	Max
-1.47947	-0.32750	-0.02448	0.30392	1.38938

Branch length transformations:

```
kappa [Fix] : 1.000
lambda [ ML] : 0.624
  lower bound : 0.000, p = 6.9777e-06
  upper bound : 1.000, p = < 2.22e-16
  95.0% CI   : (0.369, 0.809)
delta [Fix] : 1.000
```

Coefficients:

	Estimate	Std. Error	t value	Pr(> t)
(Intercept)	-3.682054	0.138500	-26.5852	< 2.2e-16 ***
log10svl	2.279498	0.075986	29.9988	< 2.2e-16 ***
h80_30	0.050417	0.012920	3.9023	0.0001385 ***

```
---
Signif. codes:  0 '***' 0.001 '**' 0.01 '*' 0.05 '.' 0.1 ' ' 1
```

Residual standard error: 0.5292 on 165 degrees of freedom
Multiple R-squared: 0.852, Adjusted R-squared: 0.8502
F-statistic: 475.1 on 2 and 165 DF, p-value: < 2.2e-16

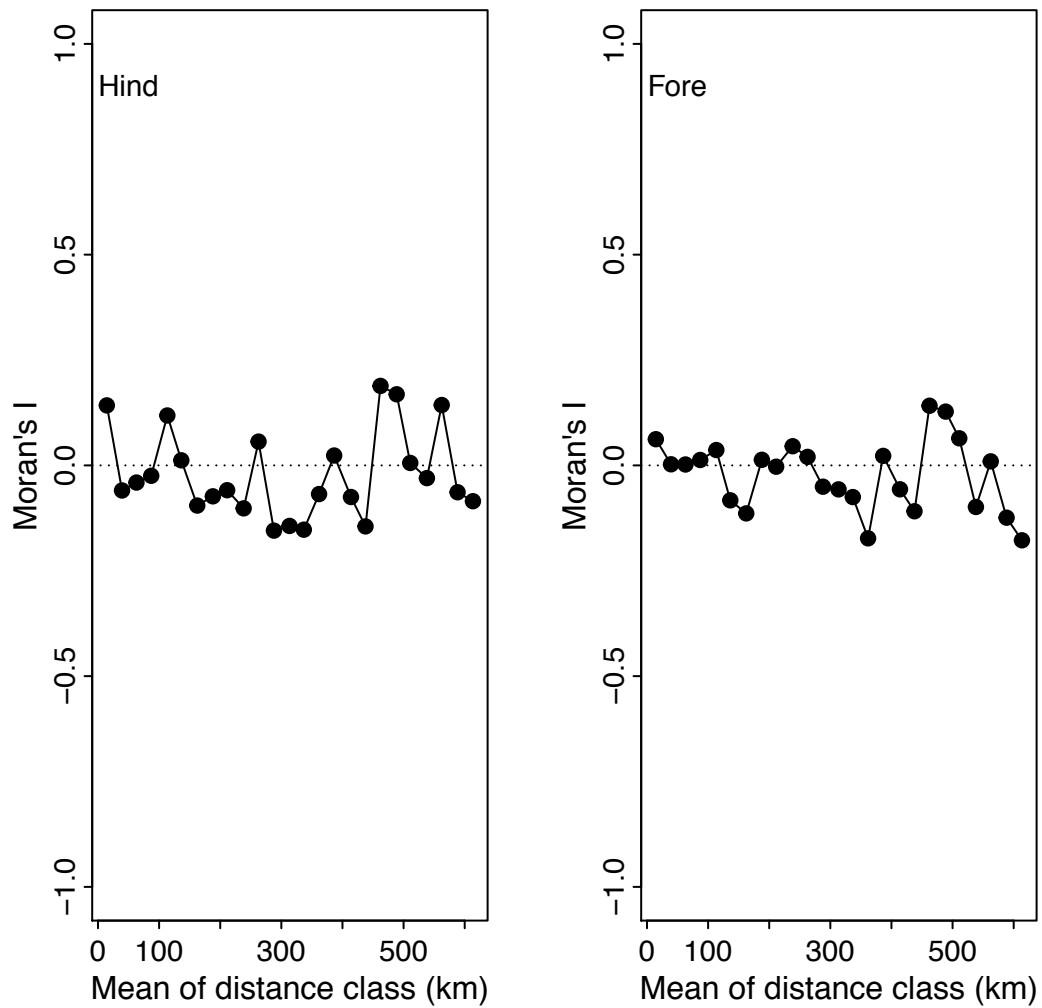


Fig. S3.1: Plot of Moran's I correlograms of hind limb toepad area (left) and forelimb toepad area (right) for all of the anole species in the dataset. We found no structure in the residuals to indicate spatial autocorrelation in the data.

Appendix 3.2: The Insular Fauna:

Mainland anoles naturally experience far fewer hurricanes than insular anoles. As a result, we analyzed solely the insular fauna in our dataset to determine if the relationship with hurricane activity was maintained, and to rule out the possibility that the mainland fauna, with its dearth of hurricane events over the period examined, was anchoring our regressions.

We determined that the insular species in our dataset had the same positive relationship with hurricane activity as seen in the genus-wide analysis presented in the manuscript.

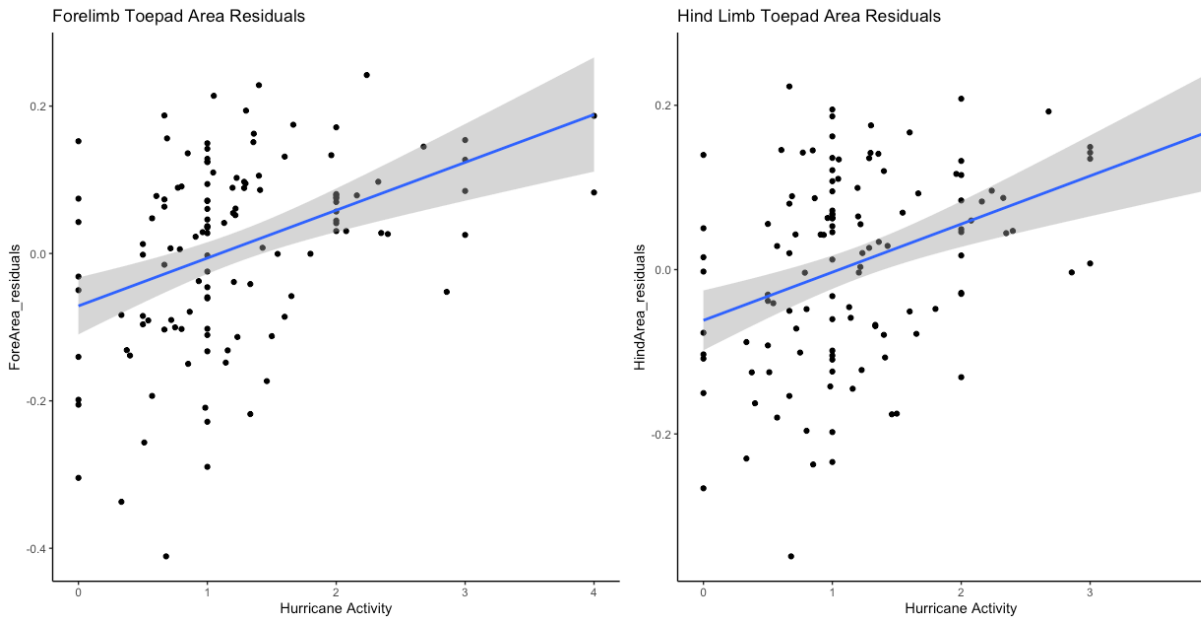


Fig. S3.2: The positive trend for the insular anoles between size-corrected forelimb (left) and hind limb (right) toepad surface area across species of different hurricane activity histories.

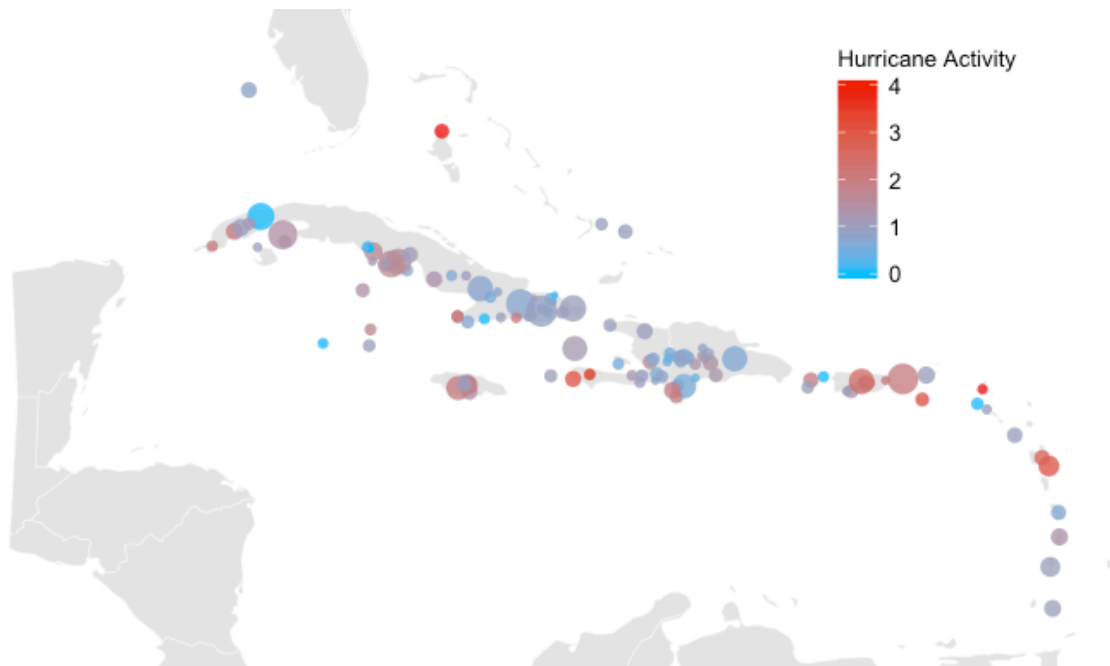


Fig. S3.3: A map showing the distribution of the insular anoles used for this analysis. Each point represents a species of anole. Point color reflects the hurricane history experienced by that species. Point size reflects the relative size of the toepads of those individuals.

Forelimb Toepad Area:

Variable codes are:

fore_area: forelimb toepad area

log10svl: log-transformed body length

h80_30: number of hurricanes exceeding 80 knots of wind within 30 km of site

```
pgls(formula = log10(fore_area) ~ log10svl + h80_30, data =  
comp_island2_toepad_data,  
lambda = "ML", kappa = 1, delta = 1, bounds = list(delta = c(1e-06,  
15)))
```

Residuals:

Min	1Q	Median	3Q	Max
-1.13797	-0.20468	0.03106	0.34670	1.29712

Branch length transformations:

```
kappa [Fix] : 1.000  
lambda [ ML] : 0.501  
  lower bound : 0.000, p = 4.5294e-05  
  upper bound : 1.000, p = 2.3315e-15  
  95.0% CI   : (0.227, 0.745)  
delta [Fix] : 1.000
```

Coefficients:

	Estimate	Std. Error	t value	Pr(> t)
(Intercept)	-4.230743	0.135325	-31.2635	< 2.2e-16 ***
log10svl	2.490762	0.075040	33.1923	< 2.2e-16 ***
h80_30	0.056232	0.012589	4.4667	1.798e-05 ***

```
---  
Signif. codes:  0 '***' 0.001 '**' 0.01 '*' 0.05 '.' 0.1 ' ' 1
```

Residual standard error: 0.4555 on 121 degrees of freedom

Multiple R-squared: 0.9066, Adjusted R-squared: 0.9051

F-statistic: 587.5 on 2 and 121 DF, p-value: < 2.2e-16

Hind Limb Toepad Area:

Variable codes are:

hind_area: hind limb toepad area

log10svl: log-transformed body length

h80_30: number of hurricanes exceeding 80 knots of wind within 30 km of site

```
pgls(formula = log10(hind_area) ~ log10svl + h80_30, data =
comp_island2_toepad_data,
      lambda = "ML", kappa = 1, delta = 1, bounds = list(delta = c(1e-06,
15)))
```

Residuals:

Min	1Q	Median	3Q	Max
-1.11777	-0.23710	0.04711	0.34731	1.18748

Branch length transformations:

```
kappa [Fix] : 1.000
lambda [ ML] : 0.383
  lower bound : 0.000, p = 0.0022307
  upper bound : 1.000, p = < 2.22e-16
  95.0% CI   : (0.109, 0.670)
delta [Fix] : 1.000
```

Coefficients:

	Estimate	Std. Error	t value	Pr(> t)
(Intercept)	-3.823156	0.125874	-30.3729	< 2.2e-16 ***
log10svl	2.365806	0.069936	33.8284	< 2.2e-16 ***
h80_30	0.047897	0.012339	3.8817	0.0001694 ***

Signif. codes: 0 '***' 0.001 '**' 0.01 '*' 0.05 '.' 0.1 ' ' 1

Residual standard error: 0.4282 on 121 degrees of freedom

Multiple R-squared: 0.9087, Adjusted R-squared: 0.9072

F-statistic: 602.5 on 2 and 121 DF, p-value: < 2.2e-16

Appendix 3.3 The Insular Fauna: Ecomorphs

Anole species in the Greater Antilles have repeatedly evolved a suite of morphologically similar types called “ecomorphs” (8, 9). Different ecomorphs specialize in different microhabitats, for example, so-called “twig” anoles have adapted to living on the thinnest branches of trees, “trunk-crown” anoles tend to spend the majority of their time where the tree trunk meets the canopy, and “trunk-ground” anoles split their time between the base of trees and the forest floor (8, 9). Ecomorphs differ in toepad characteristics with more arboreal species tending to have larger toepads (7, 8). We again examined the relationship between hurricane activity and toepad size for each of the ecomorphs to determine whether the positive relationship seen across all of the species was maintained for each ecomorph. We found that it was (Fig. S3.4, S3.5).

In order to contextualize the explanatory power of hurricanes *vis-à-vis* ecomorph class we have presented the adjusted R^2 values of three models predicting size-corrected fore- and hind limb toepad area: a full model containing both the hurricane count and ecomorph assignment, and two additional models with each factor alone. These models cannot be directly compared because the estimated phylogenetic covariance of the model’s errors will vary between models according to the factors being tested, which can have a scaling effect on the likelihood. That said, all three models indicate that hurricane activity is a significant predictor of variation in both fore- and hind limb toepads of anoles.

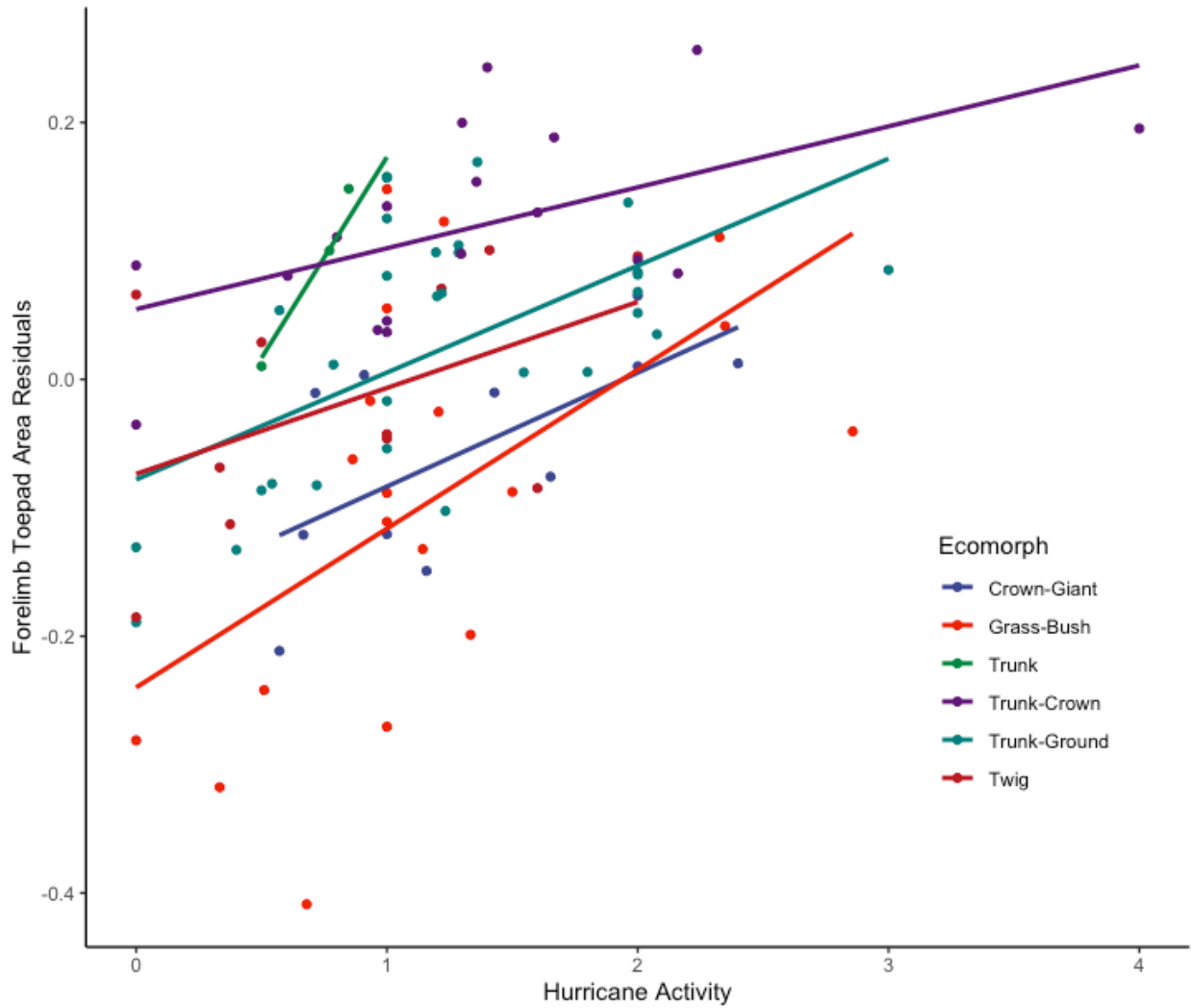


Fig. S3.4: The relationship between the size-corrected forelimb toepad surface area and hurricane activity for each of the six ecomorph classes in the Greater Antillean anole fauna. All six show a significant positive relationship with hurricane activity.

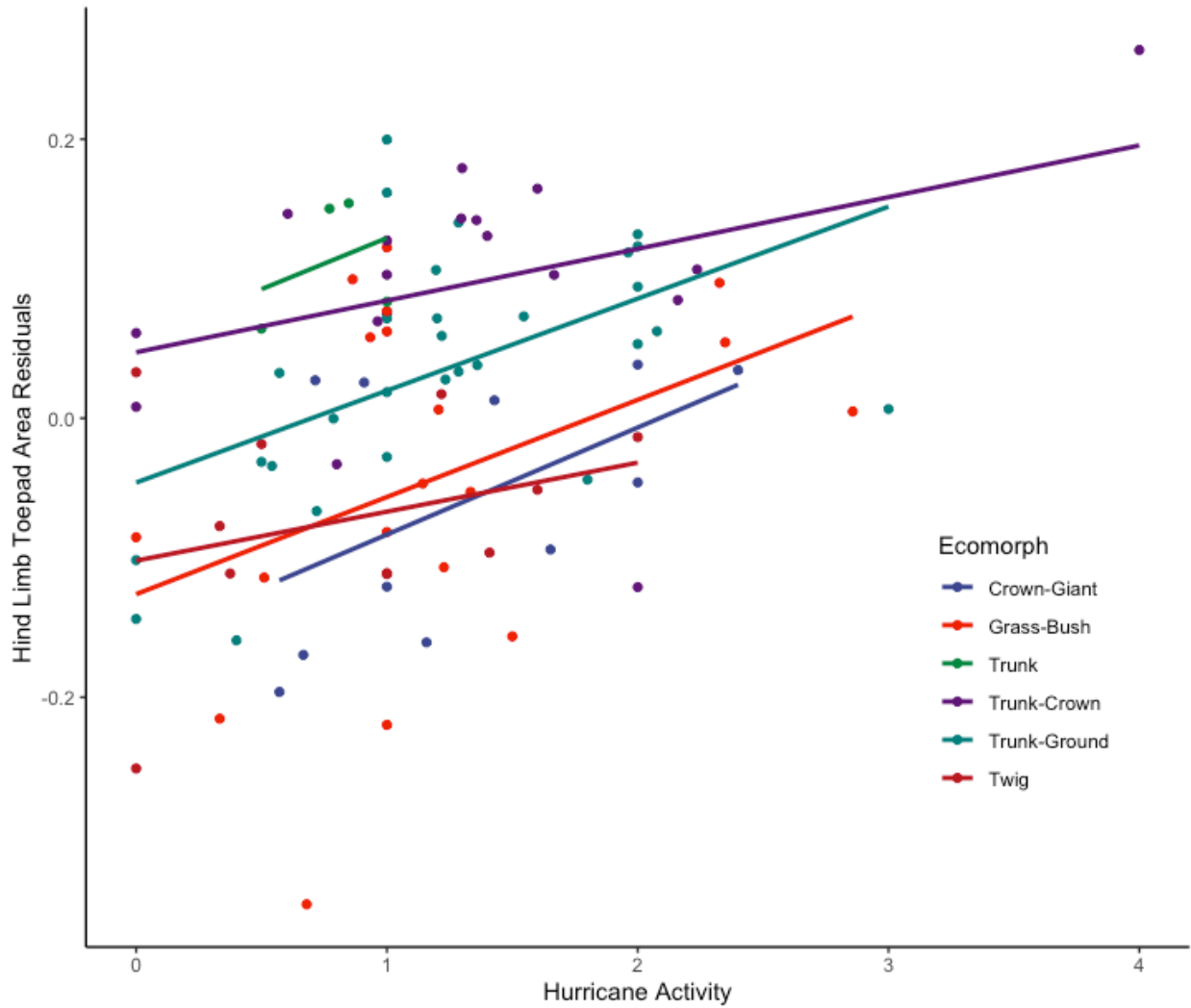


Fig. S3.5: The relationship between the size-corrected hind limb toepad surface area and hurricane activity for each of the six ecomorph classes in the Greater Antillean anole fauna. All six show a significant positive relationship with hurricane activity.

Testing for an interaction between ecomorph class and hurricane activity for forelimb toepad area:

Variable codes are:

fore_resid: body-size corrected forelimb toepad area residuals

ecomorph: categorical variable corresponding to ecomorph class

h80_30: number of hurricanes exceeding 80 knots of wind within 30 km of site

```
pgls(formula = fore_resid ~ ecomorph * h80_30, data =  
comp_ecomorph_toepad_data,  
      lambda = "ML", kappa = 1, delta = 1, bounds = list(delta = c(1e-06,  
15)))
```

Residuals:

	Min	1Q	Median	3Q	Max
	-0.67004	-0.22425	-0.04799	0.24982	0.88564

Branch length transformations:

```
kappa [Fix] : 1.000  
lambda [ ML] : 0.000  
  lower bound : 0.000, p = 1  
  upper bound : 1.000, p = < 2.22e-16  
  95.0% CI   : (NA, 0.316)  
delta [Fix] : 1.000
```

Residual standard error: 0.3505 on 80 degrees of freedom

Multiple R-squared: 0.5628, Adjusted R-squared: 0.5027

F-statistic: 9.363 on 11 and 80 DF, p-value: 1.448e-10

Analysis of Variance Table

Sequential SS for pgls: lambda = 0.00, delta = 1.00, kappa = 1.00

Response: fore_resid

	Df	Sum Sq	Mean Sq	F value	Pr(>F)
ecomorph	5	7.78	1.56	12.67	<2e-16 ***
h80_30	1	4.27	4.27	34.76	<2e-16 ***
ecomorph:h80_30	5	0.60	0.12	0.97	0.44
Residuals	80	9.83	0.12		

Signif. codes: 0 '***' 0.001 '**' 0.01 '*' 0.05 '.' 0.1 ' ' 1

Testing for an interaction between ecomorph class and hurricane activity for hind limb toepad area:

Variable codes are:

hind_resid: body-size corrected hind limb toepad area residuals

ecomorph: categorical variable corresponding to ecomorph class

h80_30: number of hurricanes exceeding 80 knots of wind within 30 km of site

```
pgls(formula = hind_resid ~ ecomorph * h80_30, data =
comp_ecomorph_toepad_data,
      lambda = "ML", kappa = 1, delta = 1, bounds = list(delta = c(1e-06,
15)))
```

Residuals:

	Min	1Q	Median	3Q	Max
	-0.53856	-0.20017	0.00711	0.26009	0.76183

Branch length transformations:

```
kappa [Fix] : 1.000
lambda [ ML] : 0.000
  lower bound : 0.000, p = 1
  upper bound : 1.000, p = < 2.22e-16
  95.0% CI : (NA, 0.332)
delta [Fix] : 1.000
```

Residual standard error: 0.346 on 80 degrees of freedom
Multiple R-squared: 0.4521, Adjusted R-squared: 0.3768
F-statistic: 6.001 on 11 and 80 DF, p-value: 4.737e-07

Analysis of Variance Table

Sequential SS for pgls: lambda = 0.00, delta = 1.00, kappa = 1.00

Response: hind_resid

	Df	Sum Sq	Mean Sq	F value	Pr(>F)
ecomorph	5	5.65	1.13	9.43	<2e-16 ***
h80_30	1	2.09	2.09	17.45	<2e-16 ***
ecomorph:h80_30	5	0.17	0.03	0.28	0.92
Residuals	80	9.58	0.12		

Signif. codes: 0 '***' 0.001 '**' 0.01 '*' 0.05 '.' 0.1 ' ' 1

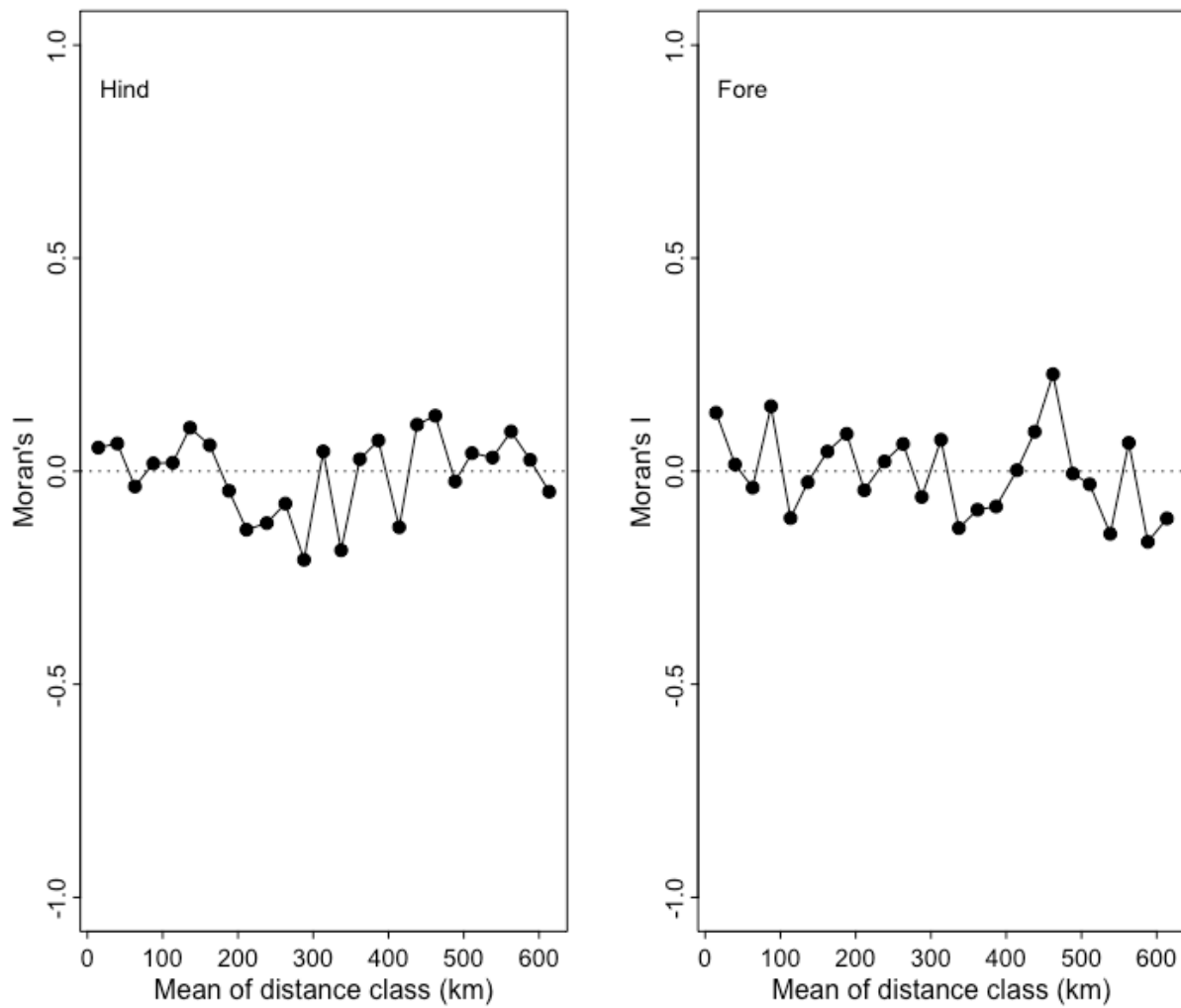


Fig. S3.6: Plot of Moran's I correlograms of hind limb toepad area (left) and forelimb toepad area (right) for the insular anole species. We found no structure in the residuals to indicate spatial autocorrelation in the data.

Appendix 4: Tree Heights

Supplemental Analysis 4.1:

Anole species that are more arboreal tend to have larger toepads (7, 8). This is a potential alternative explanation for the biogeographic patterns observed across the species in our dataset. We therefore tested whether variation in tree heights calculated using LiDAR (see Methods; 38) correlated with the observed pattern in toepad area. We found tree height was not a significant predictor of anole toepad area in this dataset.

Forelimb Toepad Area:

Variable codes are:

fore_area: forelimb toepad area

log10svl: log-transformed body length

h80_30: number of hurricanes exceeding 80 knots of wind within 30 km of site

trht.30: mean tree high within 30 km of site according to LIDAR data

```
pgls(formula = log10(fore_area) ~ log10svl + h80_30 + trht.30,
      data = comp_toepad_data, lambda = "ML", kappa = 1, delta = 1,
      bounds = list(delta = c(1e-06, 15)))
```

Residuals:

Min	1Q	Median	3Q	Max
-1.3512	-0.3695	-0.0241	0.2571	1.5543

Branch length transformations:

```
kappa [Fix] : 1.000
lambda [ ML] : 0.616
  lower bound : 0.000, p = 2.6328e-07
  upper bound : 1.000, p = 6.6613e-16
  95.0% CI    : (0.384, 0.795)
delta [Fix]  : 1.000
```

Coefficients:

	Estimate	Std. Error	t value	Pr(> t)
(Intercept)	-4.12682415	0.13193896	-31.2783	< 2.2e-16 ***
log10svl	2.42037709	0.07088469	34.1453	< 2.2e-16 ***
h80_30	0.06104561	0.01214000	5.0285	1.285e-06 ***
trht.30	0.00062595	0.00172428	0.3630	0.7171

Signif. codes: 0 '***' 0.001 '**' 0.01 '*' 0.05 '.' 0.1 ' ' 1

Residual standard error: 0.493 on 164 degrees of freedom
Multiple R-squared: 0.8833, Adjusted R-squared: 0.8811
F-statistic: 413.6 on 3 and 164 DF, p-value: < 2.2e-16

Hind Limb Toepad Area:

Variable codes are:

hind_area: hind limb toepad area

log10svl: log-transformed body length

h80_30: number of hurricanes exceeding 80 knots of wind within 30 km of site

trht.30: mean tree high within 30 km of site according to LIDAR data

```
pgls(formula = log10(hind_area) ~ log10svl + h80_30 + trht.30,
      data = comp_toepad_data, lambda = "ML", kappa = 1, delta = 1,
      bounds = list(delta = c(1e-06, 15)))
```

Residuals:

Min	1Q	Median	3Q	Max
-1.4929	-0.3342	0.0140	0.3381	1.1276

Branch length transformations:

```
kappa [Fix] : 1.000
lambda [ ML] : 0.626
  lower bound : 0.000, p = 6.7106e-06
  upper bound : 1.000, p = < 2.22e-16
  95.0% CI    : (0.371, 0.809)
delta [Fix]  : 1.000
```

Coefficients:

	Estimate	Std. Error	t value	Pr(> t)
(Intercept)	-3.66694067	0.14180056	-25.8598	< 2.2e-16 ***
log10svl	2.28001516	0.07618018	29.9292	< 2.2e-16 ***
h80_30	0.04974107	0.01300725	3.8241	0.0001862 ***
trht.30	-0.00096674	0.00185025	-0.5225	0.6020339

```
---
Signif. codes:  0 '***' 0.001 '**' 0.01 '*' 0.05 '.' 0.1 ' ' 1
```

Residual standard error: 0.5306 on 164 degrees of freedom

Multiple R-squared: 0.8522, Adjusted R-squared: 0.8495

F-statistic: 315.3 on 3 and 164 DF, p-value: < 2.2e-16

Appendix 4.1 Tree Heights and Hurricanes:

Using our dataset we investigated whether there was a relationship between hurricane frequency and average tree heights. While this is a subject for thorough future study we found that, generally, there was a negative correlation: localities with more hurricanes tended to have, on average, shorter maximum tree heights.

```
lm(formula = trht.30 ~ h80_30, data = dat_toepad)
```

Residuals:

Min	1Q	Median	3Q	Max
-18.448	-3.240	-0.106	4.308	14.741

Coefficients:

	Estimate	Std. Error	t value	Pr(> t)
(Intercept)	18.4477	0.5310	34.744	< 2e-16 ***
h80_30	-3.5198	0.4623	-7.613	7.91e-13 ***

Signif. codes: 0 '***' 0.001 '**' 0.01 '*' 0.05 '.' 0.1 ' ' 1

Residual standard error: 5.992 on 219 degrees of freedom
Multiple R-squared: 0.2093, Adjusted R-squared: 0.2057
F-statistic: 57.96 on 1 and 219 DF, p-value: 7.914e-13

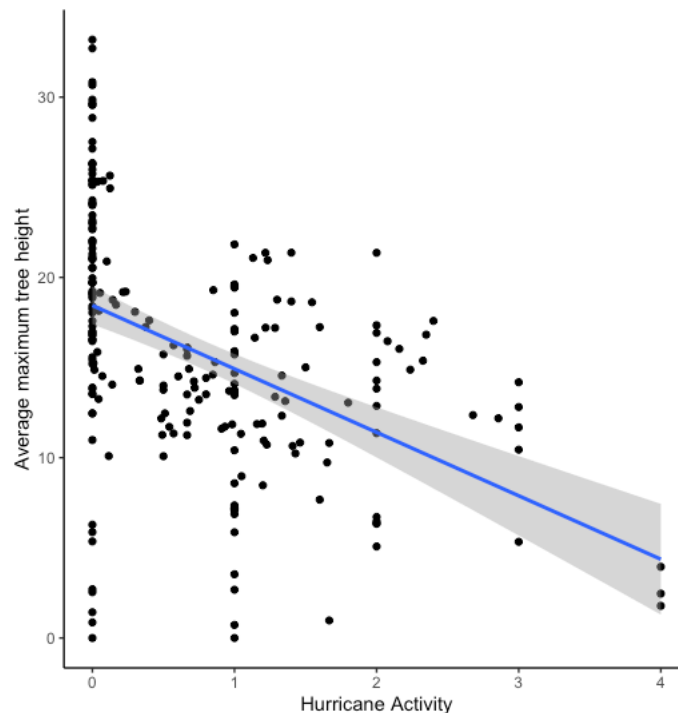


Fig 4.1: The relationship between tree height and hurricane activity was significantly negative in our dataset. Additional sampling and analysis are needed to conclusively test hurricanes' effects on vegetation structure

Appendix 5: Bioclimatic Data

We tested whether toepad size was related to air temperature or precipitation across the 188 species in our dataset. We found no relationship for either variable.

Air temperature:

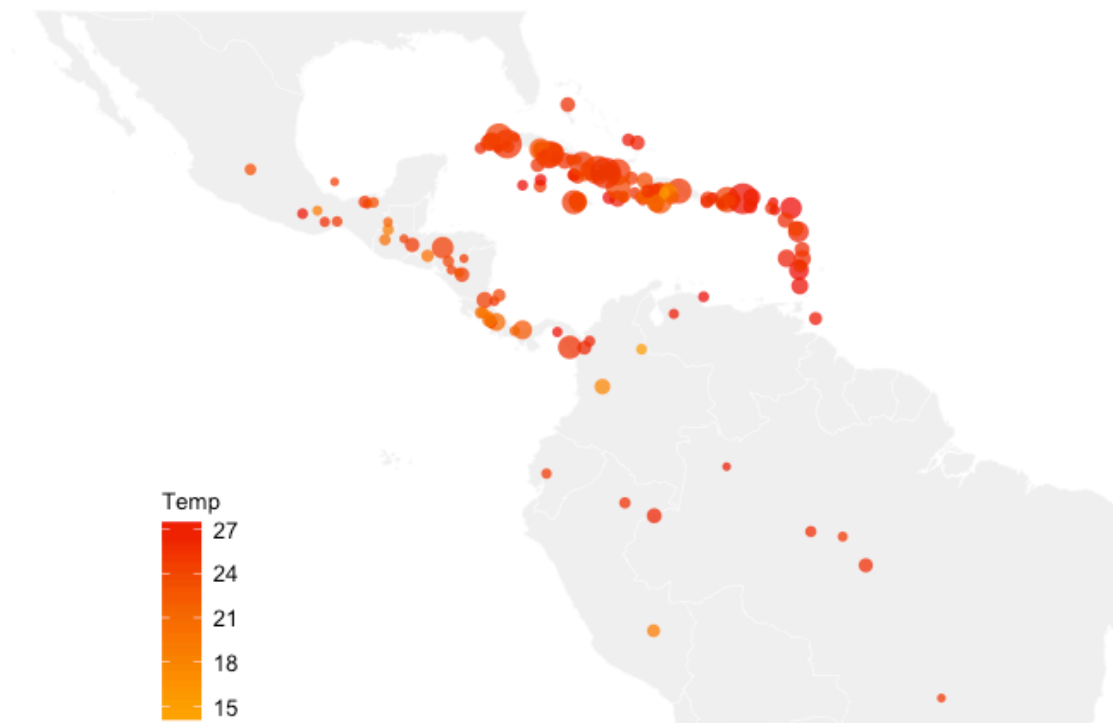


Fig. S5.1: A representation of the average mean air temperature experienced by the lizard species in this dataset. Each point corresponds to a species of anole. The size of the circle corresponds to the toepad size of that species. The color of the point corresponds to the average mean air temperature (°C).

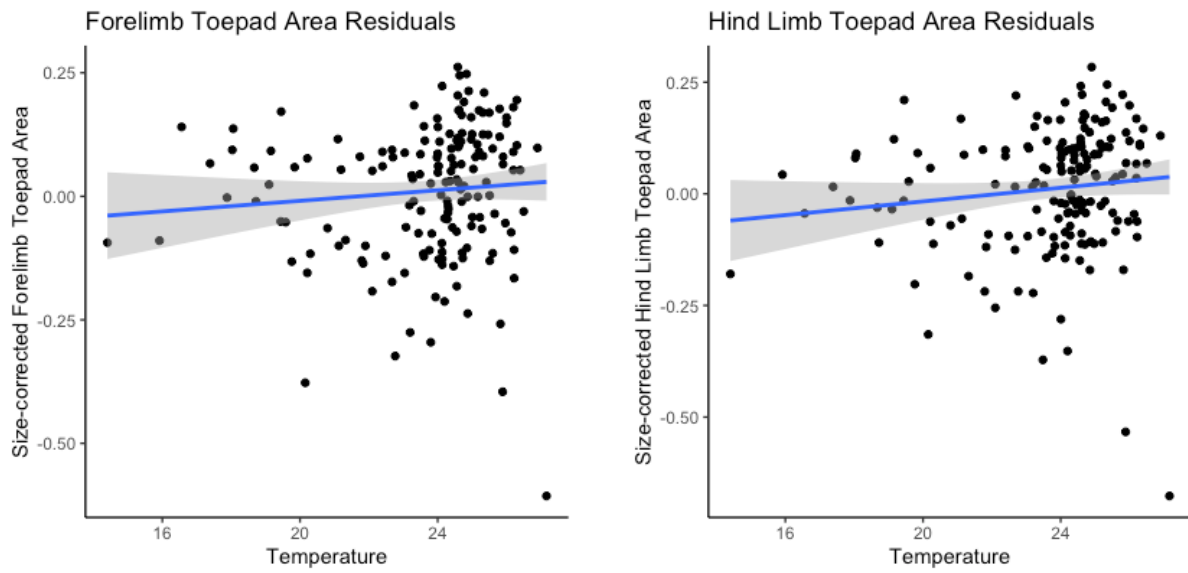


Fig. S5.2: We found no relationship between air temperature ($^{\circ}\text{C}$) and either forelimb (left) or hind limb (right) toepad surface area.

Forelimb Toepad Area:

Variable codes are:

fore_area: forelimb toepad area

log10svl: log-transformed body length

Temp: mean annual air temperature at site

```
pgls(formula = log10(fore_area) ~ log10svl + Temp, data = comp_toepad_data,
      lambda = "ML", kappa = 1, delta = 1, bounds = list(delta = c(1e-06,
15)))
```

Residuals:

Min	1Q	Median	3Q	Max
-1.60561	-0.31937	-0.00097	0.32683	1.18628

Branch length transformations:

```
kappa [Fix] : 1.000
lambda [ ML] : 0.672
  lower bound : 0.000, p = 4.3931e-10
  upper bound : 1.000, p = 9.2593e-14
  95.0% CI   : (0.460, 0.834)
delta [Fix] : 1.000
```

Coefficients:

	Estimate	Std. Error	t value	Pr(> t)
(Intercept)	-4.16807382	0.16764639	-24.8623	<2e-16 ***
log10svl	2.45190636	0.07698547	31.8490	<2e-16 ***
Temp	0.00020803	0.00047748	0.4357	0.6636

Signif. codes: 0 '***' 0.001 '**' 0.01 '*' 0.05 '.' 0.1 ' ' 1

Residual standard error: 0.5386 on 165 degrees of freedom

Multiple R-squared: 0.8627, Adjusted R-squared: 0.8611

F-statistic: 518.5 on 2 and 165 DF, p-value: < 2.2e-16

Hind Limb Toepad Area:

Variable codes are:

hind_area: hind limb toepad area

log10svl: log-transformed body length

Temp: mean annual air temperature at site

```
pgls(formula = log10(hind_area) ~ log10svl + Temp, data = comp_toepad_data,
      lambda = "ML", kappa = 1, delta = 1, bounds = list(delta = c(1e-06,
      15)))
```

Residuals:

Min	1Q	Median	3Q	Max
-1.20185	-0.44473	0.01279	0.36158	2.10072

Branch length transformations:

```
kappa [Fix] : 1.000
lambda [ ML] : 0.688
  lower bound : 0.000, p = 1.4217e-09
  upper bound : 1.000, p = 2.9976e-15
  95.0% CI   : (0.469, 0.845)
delta [Fix] : 1.000
```

Coefficients:

	Estimate	Std. Error	t value	Pr(> t)
(Intercept)	-3.81321748	0.17492200	-21.7995	<2e-16 ***
log10svl	2.29686973	0.08025691	28.6190	<2e-16 ***
Temp	0.00061996	0.00049732	1.2466	0.2143

```
---
Signif. codes:  0 '***' 0.001 '**' 0.01 '*' 0.05 '.' 0.1 ' ' 1
```

Residual standard error: 0.5636 on 165 degrees of freedom
Multiple R-squared: 0.8366, Adjusted R-squared: 0.8347
F-statistic: 422.5 on 2 and 165 DF, p-value: < 2.2e-16

Precipitation:

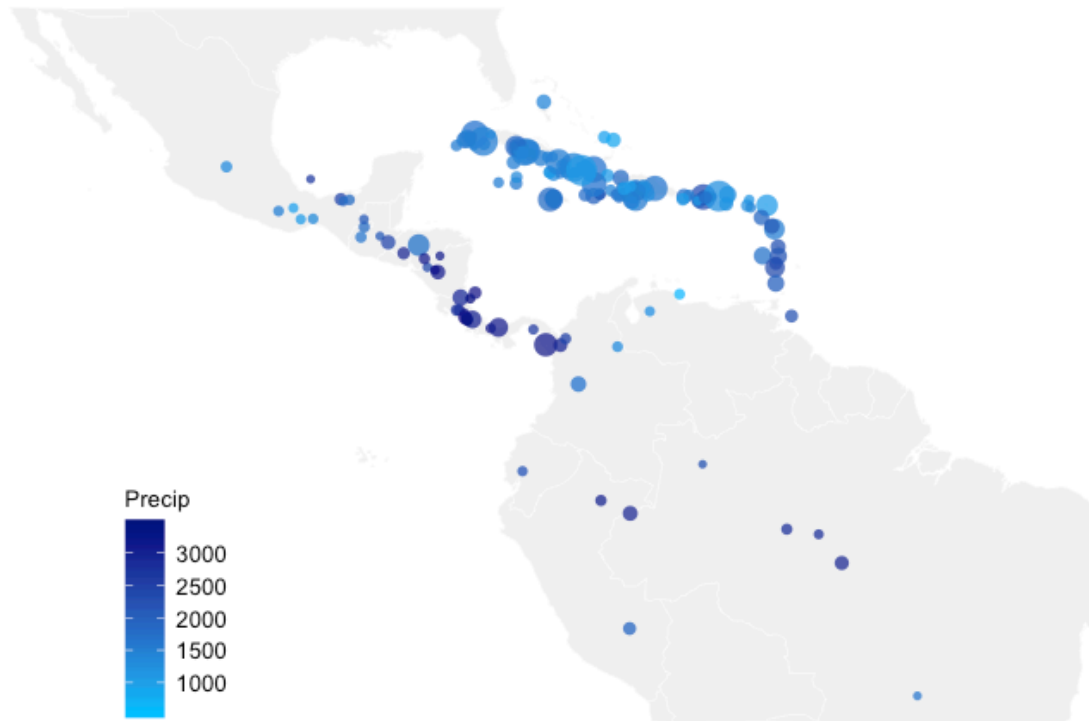


Fig. S5.3: A representation of the average of annual mean precipitation experienced by the lizard species in this dataset. Each point corresponds to a species of anole. The size of the circle corresponds to the toepad size of that species. The color of the point corresponds to the average mean precipitation (mm)

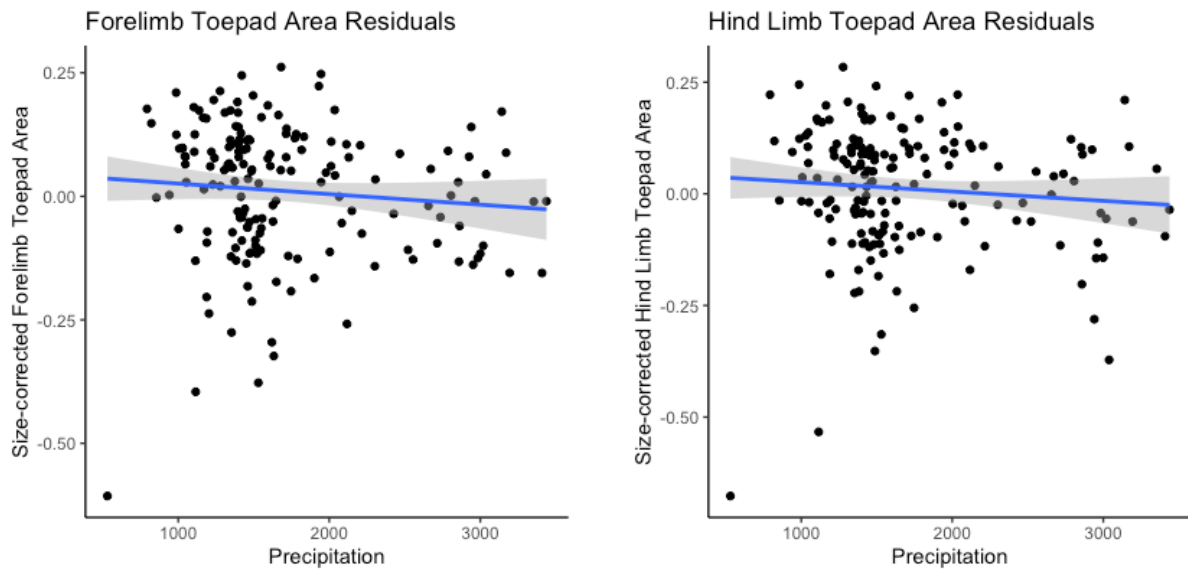


Fig. S5.4: We found no relationship between precipitation (mm) and either forelimb (left) or hind limb (right) toepad surface area.

Forelimb Toepad Area:

Variable codes are:

fore_area: forelimb toepad area

log10svl: log-transformed body length

Precip: Mean annual precipitation at site

```
pgls(formula = log10(fore_area) ~ log10svl + Precip, data = comp_toepad_data,
      lambda = "ML", kappa = 1, delta = 1, bounds = list(delta = c(1e-06,
      15)))
```

Residuals:

Min	1Q	Median	3Q	Max
-1.26611	-0.34229	-0.06379	0.29962	2.18959

Branch length transformations:

```
kappa [Fix] : 1.000
lambda [ ML] : 0.688
  lower bound : 0.000, p = 3.2091e-10
  upper bound : 1.000, p = 1.853e-13
  95.0% CI   : (0.479, 0.845)
delta [Fix] : 1.000
```

Coefficients:

	Estimate	Std. Error	t value	Pr(> t)
(Intercept)	-4.1607e+00	1.4396e-01	-28.9020	<2e-16 ***
log10svl	2.4514e+00	7.6479e-02	32.0528	<2e-16 ***
Precip	2.3973e-05	2.3418e-05	1.0237	0.3075

Signif. codes: 0 '***' 0.001 '**' 0.01 '*' 0.05 '.' 0.1 ' ' 1

Residual standard error: 0.541 on 165 degrees of freedom

Multiple R-squared: 0.8626, Adjusted R-squared: 0.8609

F-statistic: 518 on 2 and 165 DF, p-value: < 2.2e-16

Hind Limb Toepad Area:

Variable codes are:

hind_area: hind limb toepad area

log10svl: log-transformed body length

Precip: mean annual precipitation at site

```
pgls(formula = log10(hind_area) ~ log10svl + Precip, data = comp_toepad_data,
      lambda = "ML", kappa = 1, delta = 1, bounds = list(delta = c(1e-06,
15)))
```

Residuals:

Min	1Q	Median	3Q	Max
-1.53539	-0.38082	0.01389	0.39747	1.85101

Branch length transformations:

```
kappa [Fix] : 1.000
lambda [ ML] : 0.696
  lower bound : 0.000, p = 1.1855e-09
  upper bound : 1.000, p = 4.6629e-15
  95.0% CI   : (0.479, 0.850)
delta [Fix] : 1.000
```

Coefficients:

	Estimate	Std. Error	t value	Pr(> t)	
(Intercept)	-3.7231e+00	1.5062e-01	-24.7194	<2e-16	***
log10svl	2.3060e+00	7.9997e-02	28.8256	<2e-16	***
Precip	2.1404e-05	2.4513e-05	0.8731	0.3839	

```
---
Signif. codes:  0 '***' 0.001 '**' 0.01 '*' 0.05 '.' 0.1 ' ' 1
```

Residual standard error: 0.5668 on 165 degrees of freedom

Multiple R-squared: 0.8354, Adjusted R-squared: 0.8334

F-statistic: 418.8 on 2 and 165 DF, p-value: < 2.2e-16

Appendix 6: Sensitivity Analysis

For our main-text analyses, we counted a hurricane strike if it passed within 30 km of a lizard locality in our spatial dataset with maximum wind speed at or exceeding 80 knots. To determine how sensitive our model was to these two parameters we adjusted our algorithm to count hurricanes at larger radii and different windspeed threshold cutoffs. In general, larger distance thresholds showed smaller effects on the toepads of lizards. Another general pattern was that higher intensity thresholds had a more significant effect than lower thresholds.

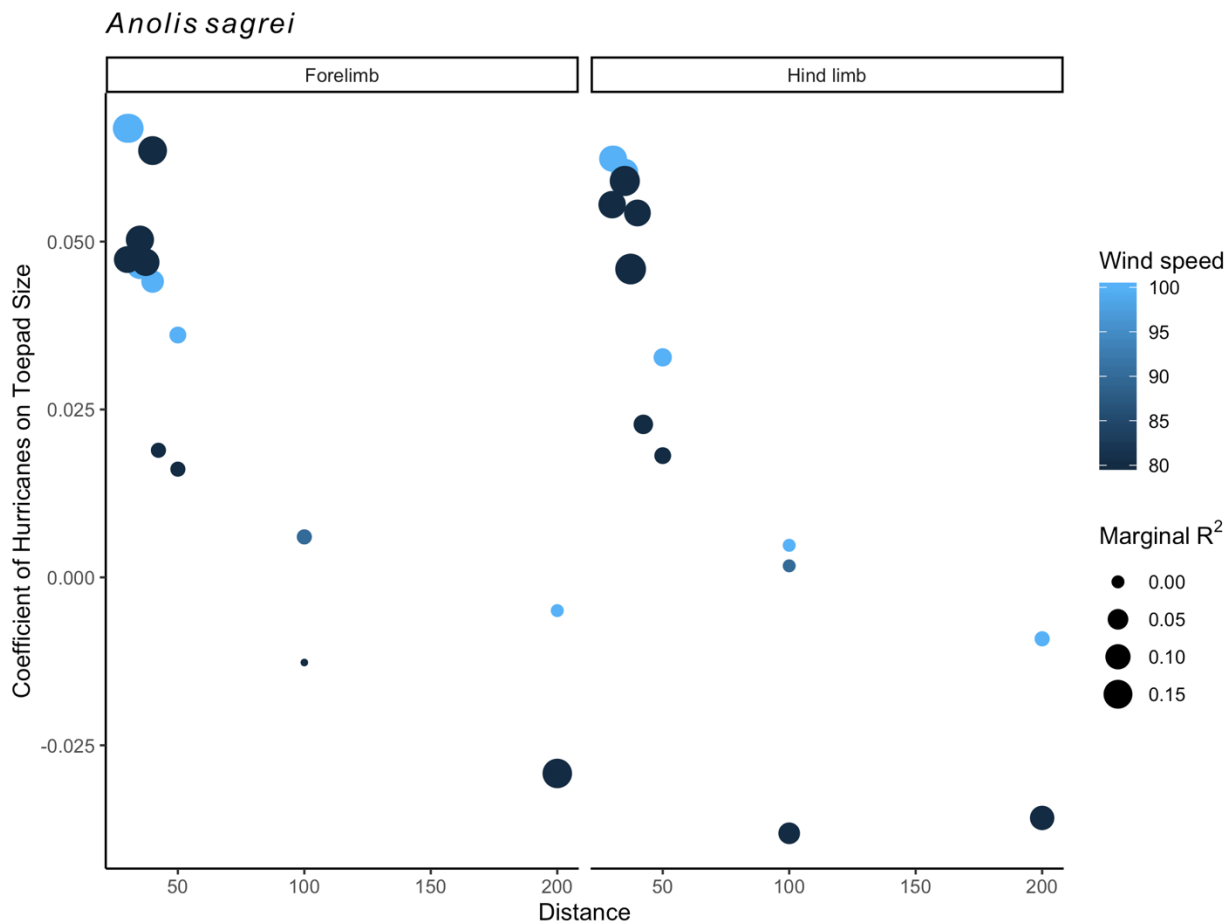


Fig. S6.1: *Anolis sagrei* sensitivity to hurricane distance and windspeed thresholds.

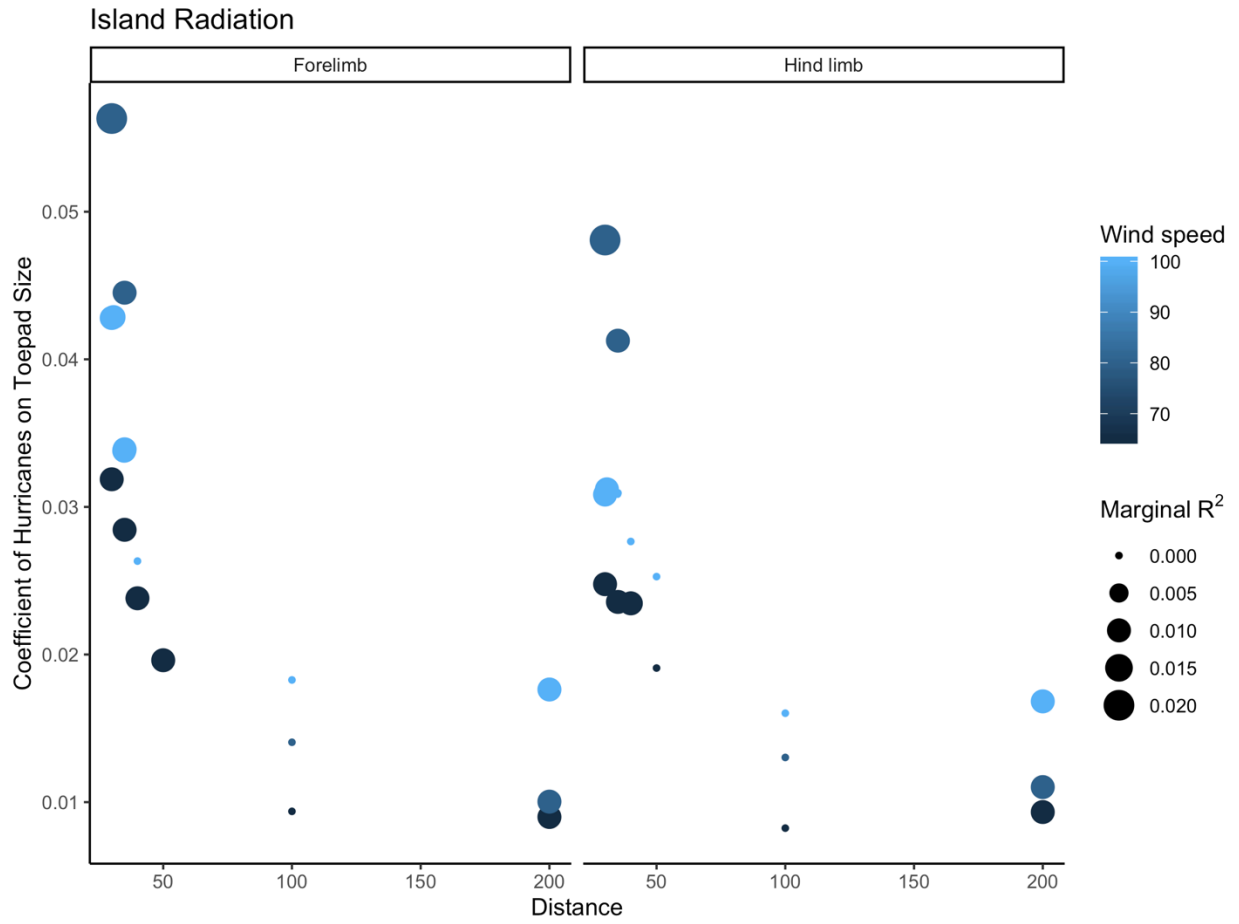


Fig. S6.2: Sensitivity of insular anoles to hurricane distance and windspeed thresholds.

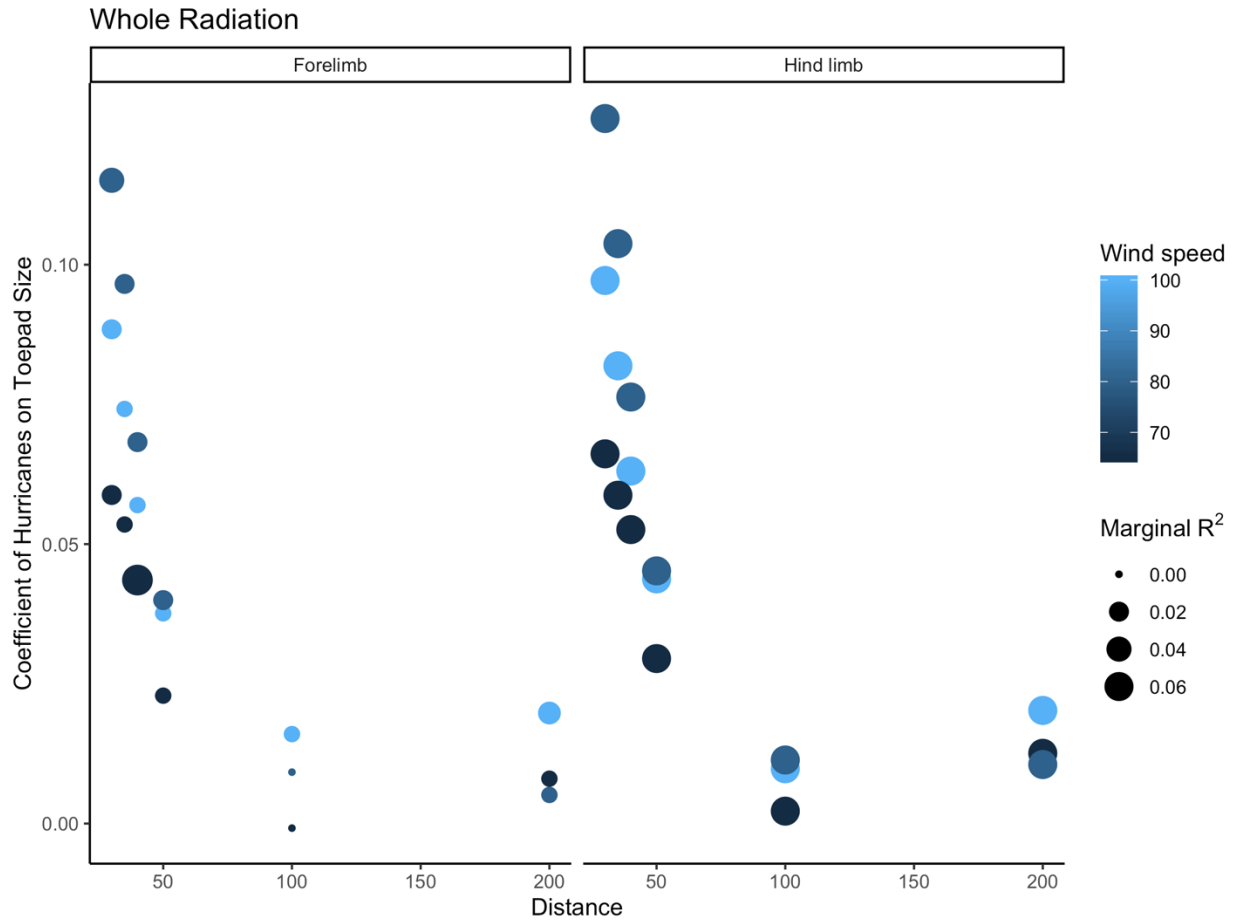


Fig. S6.3: Sensitivity of the entire genus model to hurricane distance and windspeed thresholds.

Appendix 7: Species Sampling

Because widespread species are only represented by three individuals in this dataset, it is possible that those individuals were from a population that does not best reflect the hurricane history of that species. While these potential mismatches should increase variation and thus decrease the strength of the regression, we tested whether excluding especially widespread species affected the conclusions of our macroevolutionary comparison. For this restricted analysis we excluded: *A. carolinensis*, *A. sagrei*, *A. distichus*, *A. cybotes*, *A. porcatus*, *A. cristatellus*, and *A. biporcatus*. We found that restricting these widespread species did not change the qualitative patterns of the results and, as predicted, increased the strength of the relationship. For the manuscript analysis we relate the results of the full model including the seven widespread species.

Forelimb toepads:

Variable codes are:

fore_area: forelimb toepad area

log10svl: log-transformed body length

h80_30: number of hurricanes exceeding 80 knots of wind within 30 km of site

```
pgls(formula = log10(fore_area) ~ log10svl + h80_30, data = comp_toepad_data,  
      lambda = "ML", kappa = 1, delta = 1, bounds = list(delta = c(1e-06,  
15)))
```

Residuals:

Min	1Q	Median	3Q	Max
-1.3175	-0.3636	-0.0230	0.3492	1.3646

Branch length transformations:

```
kappa [Fix] : 1.000  
lambda [ ML] : 0.609  
  lower bound : 0.000, p = 1.1903e-06  
  upper bound : 1.000, p = 1.9984e-15  
  95.0% CI   : (0.366, 0.796)  
delta [Fix] : 1.000
```

Coefficients:

	Estimate	Std. Error	t value	Pr(> t)
(Intercept)	-4.102809	0.131694	-31.1541	< 2.2e-16 ***
log10svl	2.412324	0.072412	33.3141	< 2.2e-16 ***
h80_30	0.060345	0.012325	4.8961	2.383e-06 ***

```
---  
Signif. codes:  0 '***' 0.001 '**' 0.01 '*' 0.05 '.' 0.1 ' ' 1
```

Residual standard error: 0.4962 on 159 degrees of freedom
Multiple R-squared: 0.8814, Adjusted R-squared: 0.8799
F-statistic: 590.7 on 2 and 159 DF, p-value: < 2.2e-16

Hind limb toepads:

Variable codes are:

hind_area: hind limb toepad area

log10svl: log-transformed body length

h80_30: number of hurricanes exceeding 80 knots of wind within 30 km of site

```
pgls(formula = log10(hind_area) ~ log10svl + h80_30, data = comp_toepad_data,
      lambda = "ML", kappa = 1, delta = 1, bounds = list(delta = c(1e-06,
15)))
```

Residuals:

Min	1Q	Median	3Q	Max
-1.98097	-0.28502	-0.00109	0.32048	1.55236

Branch length transformations:

```
kappa [Fix] : 1.000
lambda [ ML] : 0.605
  lower bound : 0.000, p = 3.6719e-05
  upper bound : 1.000, p = < 2.22e-16
  95.0% CI   : (0.335, 0.802)
delta [Fix] : 1.000
```

Coefficients:

	Estimate	Std. Error	t value	Pr(> t)	
(Intercept)	-3.677753	0.141471	-25.9966	< 2.2e-16	***
log10svl	2.276742	0.077794	29.2663	< 2.2e-16	***
h80_30	0.050536	0.013255	3.8127	0.0001963	***

Signif. codes: 0 '***' 0.001 '**' 0.01 '*' 0.05 '.' 0.1 ' ' 1

Residual standard error: 0.5329 on 159 degrees of freedom

Multiple R-squared: 0.8505, Adjusted R-squared: 0.8486

F-statistic: 452.3 on 2 and 159 DF, p-value: < 2.2e-16

Appendix 8: MATLAB code for calculating hurricane strikes.

Data sources:

Tropical cyclone track data from 1851-2016 (North Atlantic) and 1949-2016 (Eastern North Pacific) are obtained from the International Best Track Archive for Climate Stewardship (IBTrACS). These data are available at:

<https://www.ncdc.noaa.gov/ibtracs/index.php?name=ibtracs-data>

When we obtained the tracks, IBTrACS data were not available for 2017. Therefore, we obtained 2017 North Atlantic and Eastern Pacific tracks from the tropical cyclone extended best track dataset:

http://rammb.cira.colostate.edu/research/tropical_cyclones/tc_extended_best_track_dataset/

In both datasets, data are provided at 6-hour intervals at 0000, 0600, 1200, and 1800 UTC. Sometimes, data between these 6-hr points are provided for special events in the tropical cyclone lifecycle (usually landfall).

Interpolation:

Before calculating the number of hurricane strikes at each location, we interpolated the data to 15-minute frequency. To do this, the TC position between two time points (e.g. 0000 UTC and 0600 UTC) was interpolated to 23 15-minute time points between these two times (0015 UTC, 0030 UTC, ..., 0530 UTC, 0545 UTC).

The reason for interpolating between time points is to avoid instances where storms “skip over” a location. For example, say we are determining whether a storm passes within 30 km of a specific location. At 0000 UTC, the storm is 40 km east of the location. At 0600 UTC, the storm

is 40 km west of the location. But this hypothetical storm passes over the location between these two times, so we want it recognized. Thus, we interpolate to time points between 0000 UTC and 0600 UTC.

As noted above, there are some time points that fall between 6-hour intervals. We did not remove these time points, as they give precise landfall locations. Therefore, interpolations involving these time points provide data at intervals shorter than 15 minutes.

Note that this method may technically miss some very marginal data, for example, if a storm is 30.01 km from a chosen location at 0445 UTC and at 0500 UTC, but only 29.99 km from the location at 0452 UTC. In this case, the storm would not be considered a “hit” within 30 km. However, practically, it is impossible to estimate tropical cyclone position with that level of precision.

Wind speed interpolation

Wind speed data are also provided at 6-hour intervals (and sometime also at landfall times). Typically, tropical cyclone wind speed is taken as the wind speed at the most recent time point. (e.g. the wind speed at 0500 UTC is given as the wind speed at 0000 UTC, not the wind speed at 0600 UTC).

This typical analysis method can cause problems for storms that strengthen/weaken rapidly, especially when making landfall. Therefore, we interpolated both the storm position and wind speed between time points.

Interpolation code:

```
clear  
  
test=load('NATL_1851.m');  
size1=size(test);
```



```

rows=size1(1);
rml=rows-1;
inum=24;

testcell=mat2cell(test,rows,7);

for n = 1:rml
% n = 1:rml
    if testcell{1}(n,3)==testcell{1}(n+1,3) &
testcell{1}(n,2)==testcell{1}(n+1,2)
        for o=1:inum
            intcell{1}(n*24-(24-o),1:7)=testcell{1}(n,1:7)*(24-
o+1)/24+testcell{1}(n+1,1:7)*(o-1)/24
        end
    else
        intcell{1}(n*24-23,:)=testcell{1}(n,:);
    end
end
intcell{1}(n*24+1,:)=testcell{1}(n+1,:)*(24)/24;

intmat=intcell{1};

TF1=intmat(:,1)==0 & intmat(:,2)==0 & intmat(:,3)==0 & intmat(:,4)==0 &
intmat(:,5)==0;

intmat(TF1,:)=[];
NATL_int15min_wwind=intmat;

save('NATL_interp15m_wwind','NATL_int15min_wwind')

```

Threshold counting code:

```

clear

pir=3.1415926535/180;

%Set minimum wind speed threshold (kt)
WT=100;
%Set maximum distance threshold (km)
DT=30;

locs=load('.../.../.../Anole_locs.m');
load('.../.../.../Data_1949.mat');
TCs=NATL_int15min_1949;
sizeTCs=size(TCs);
rowTCs=sizeTCs(1);
sizelocs=size(locs);
rowlocs=sizelocs(1);
collocs=sizelocs(2);
locscell=mat2cell(locs,rowlocs,collocs);

%for m=1:rowlocs
for m=1:rowlocs
for n=1:rowTCs

dist(n,1)=acos(sin((locscell{:}(m,2))*pir)*sin((TCs(n,4))*pir)+cos((locscell{
{:}(m,2))*pir)*cos((TCs(n,4))*pir)*cos((TCs(n,5))*pir-
(locscell{:}(m,1))*pir))*6371;

```

```

end

TC_dist1=TCs;
TC_dist1(:,8)=dist;
TCd=TC_dist1;

%sumtest=sum(TC_dist1{:}(:,6) > 79 & TC_dist1{:}(:,8) < 500)
%EXT_test= TC_dist1((TC_dist1{:}(:,6) > 79 & (TC_dist1{:}(:,8) < 500),:);
Ext=TCd((TCd(:,6)>=WT) & (TCd(:,8)<=DT),:);

C=unique(Ext(:,2:3), 'rows');
sizeC=size(C);
numstorm=sizeC(1)

% Next print value (but to a cell array or matrix?)

A_1949_100_30(m,1)=numstorm;

end
save('NATL_1949_nowind', 'A_1949_100_30', '-append')

```

Combining all output files into a final hurricane count dataset:

```

clear

load('NATL_1949_nowind.mat');
load('../..//ENP/No_wind/ENP_1949_nowind.mat')

T_100_30=A_1949_100_30+E_1949_100_30;
T_100_35=A_1949_100_35+E_1949_100_35;
T_100_40=A_1949_100_40+E_1949_100_40;
T_100_50=A_1949_100_50+E_1949_100_50;
T_100_100=A_1949_100_100+E_1949_100_100;
T_100_200=A_1949_100_200+E_1949_100_200;

T_90_30=A_1949_90_30+E_1949_90_30;
T_90_35=A_1949_90_35+E_1949_90_35;
T_90_40=A_1949_90_40+E_1949_90_40;
T_90_50=A_1949_90_50+E_1949_90_50;
T_90_100=A_1949_90_100+E_1949_90_100;
T_90_200=A_1949_90_200+E_1949_90_200;

T_80_30=A_1949_80_30+E_1949_80_30;
T_80_35=A_1949_80_35+E_1949_80_35;
T_80_40=A_1949_80_40+E_1949_80_40;
T_80_50=A_1949_80_50+E_1949_80_50;
T_80_100=A_1949_80_100+E_1949_80_100;
T_80_200=A_1949_80_200+E_1949_80_200;

T_80_3731_3110=A_1949_80_3731+E_1949_80_3110;
T_80_4232_3110=A_1949_80_4232+E_1949_80_3110;

T_90_3294_3045=A_1949_90_3294+E_1949_90_3045;
T_90_3764_3045=A_1949_90_3764+E_1949_90_3045;

T_100_3072_2969=A_1949_100_3072+E_1949_100_2969;

```

```
T_100_3486_2969=A_1949_100_3486+E_1949_100_2969;

Num_liz_comb=[T_80_30,T_80_35,T_80_40,T_80_50,T_80_100,T_80_200,T_90_30,T_90_
35,T_90_40,T_90_50,T_90_100,T_90_200,T_100_30,T_100_35,T_100_40,T_100_50,T_10
0_100,T_100_200,T_80_3731_3110,T_80_4232_3110,T_90_3294_3045,T_90_3764_3045,T
_100_3072_2969,T_100_3486_2969];

dlmwrite('Data_Total_1949_Nowind.txt',Num_liz_comb)

clear
```